

Pulling Target to Source: A New Perspective on Domain Adaptive Semantic Segmentation

Haochen Wang^{1,2} Yujun Shen³ Jingjing Fei⁴ Wei Li⁴ Liwei Wu⁴
 Yuxi Wang^{1,5} Zhaoxiang Zhang^{1,2,5*}

¹Center for Research on Intelligent Perception and Computing,

National Laboratory of Pattern Recognition, Institute of Automation, Chinese Academy of Sciences

²University of Chinese Academy of Sciences ³CUHK ⁴SenseTime Research

⁵Centre for Artificial Intelligence and Robotics,
 Hong Kong Institute of Science & Innovation, Chinese Academy of Science

{wanghaochen2022, zhaoxiang.zhang}@ia.ac.cn {shenyujun0302, yuxiwang93}@gmail.com
 {feijingjing1, liwei1, wuliwei}@sensetime.com

Abstract

Domain adaptive semantic segmentation aims to transfer knowledge from a labeled source domain to an unlabeled target domain. However, existing methods primarily focus on directly learning qualified target features, making it challenging to guarantee their discrimination in the absence of target labels. This work provides a new perspective. We observe that the features learned with source data manage to keep categorically discriminative during training, thereby enabling us to implicitly learn adequate target representations by simply **pulling target features close to source features for each category**. To this end, we propose T2S-DA, which we interpret as a form of pulling Target to Source for Domain Adaptation, encouraging the model in learning similar cross-domain features. Also, considering the pixel categories are heavily imbalanced for segmentation datasets, we come up with a dynamic re-weighting strategy to help the model concentrate on those underperforming classes. Extensive experiments confirm that T2S-DA learns a more discriminative and generalizable representation, significantly surpassing the state-of-the-art. We further show that our method is quite qualified for the domain generalization task, verifying its domain-invariant property.¹

1. Introduction

The success of semantic segmentation largely relies on big data [39, 57, 80], however, collecting a sufficient number of annotated images could be labor-intensive in practice [11, 82]. Recent studies [79, 26, 1, 23] yield an alternative

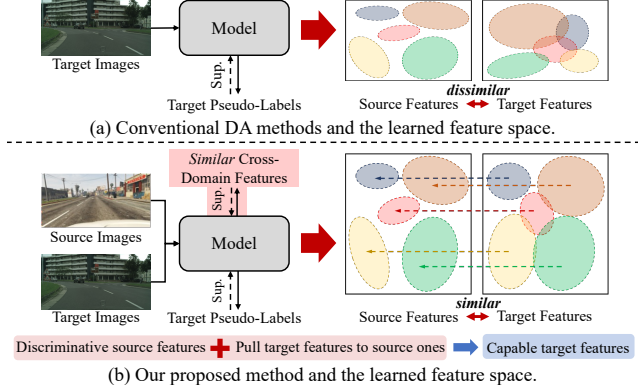


Figure 1. **Concept comparison** between (a) conventional methods and (b) our T2S-DA. To obtain discriminative features from target images, existing approaches *directly* supervise the model with target pseudo-labels regardless of the similarity between cross-domain features. Differently, T2S-DA addresses this issue from a new perspective, where we argue that “discriminative source features” plus “making target features close to source features” *implicitly* brings capable target features.

solution by introducing synthetic datasets [56, 58], where the labels can be obtained with minor effort. However, the models learned on these datasets are found hard to generalize to real-world scenarios. To address this challenge, unsupervised domain adaptation (UDA) [84, 67, 38] is proposed to transfer knowledge from the labeled source domain (*e.g.*, synthetic) to an unlabeled target domain (*e.g.*, real). Under this setting, the crux becomes how to make full use of source labels to learn discriminative representations for segmenting target samples.

To address this issue, typical solutions fall into two categories, *i.e.*, adversarial training, and self-training. The former tries to align the feature distribution of different

*Corresponding author.

¹Code will be made publicly available.

domains to an *intermediate common space* [17, 49, 65, 44, 7, 66, 52, 73, 43, 16, 41]. Although these approaches converge the two domains globally, it is hard to ensure that target features from different categories are well-separated [74, 14]. The latter aims to build a capable target feature space by selecting confident target predictions as pseudo-ground truths [64, 85, 78, 79, 34, 81, 1, 61, 14, 77, 76, 70]. These approaches *directly* supervise the model with target pseudo-labels. But the segmentation model usually tends to be biased to the source domain, resulting in error-prone target pseudo-labels [34].

We argue that *the performance deterioration is highly related to the feature dissimilarity*, and thus this work focuses on *explicitly* minimizing the domain discrepancy. A straightforward way is to learn source features in the target style, *i.e.*, “source \rightarrow target”, but we empirically find that it is hard to build categorical discriminative target features through this way (see Sec. 4.2). Therefore, we propose to *pull target to source*. Thanks to the supervision of source labels, source features are *always* qualified during training. Therefore, regarding source features as anchors, then simply *pulling target features close to source ones*, implicitly improves the capability of target features. In other words, as illustrated in Fig. 1, we argue that “discriminative source features” plus “pulling target features close to source ones” contributes to a category-discriminative target feature space. However, due to the lack of target labels, it is hard to conduct feature pairs that *exactly* belong to the same class.

To this end, we propose T2S-DA. In particular, we introduce an image translation engine to produce pseudo-images by transferring source data to the target style. These pseudo-images are then served as queries and can be easily matched with their positive keys (*i.e.*, source features from the same category) *precisely* since they naturally have annotations. Additionally, considering the pixel categories are heavily imbalanced for segmentation datasets, we put forward a dynamic re-weighting strategy, forcing the model to put more effort into those underperforming classes. Through this way, our approach is able to learn similar representations across domains and hence achieves substantial improvements on the target domain. From Fig. 2, we can tell that *the improved similarity indeed contributes to better performances*, especially for class `train`.

We evaluate the proposed T2S-DA on two UDA benchmarks, *i.e.*, GTA5 [56] \rightarrow Cityscapes [11] and SYNTHIA [58] \rightarrow Cityscapes [11], where we consistently surpass existing alternatives. For instance, T2S-DA achieves 75.1% mIoU [15] on GTA5 \rightarrow Cityscapes benchmark, outperforming the state-of-the-art alternative, *i.e.*, HRDA [24] by +1.3%. Moreover, we find T2S-DA is also applicable to the domain generalization task, where the training phase cannot access the target samples at all. Under this setting, when training the model on GTA5 and SYNTHIA and testing

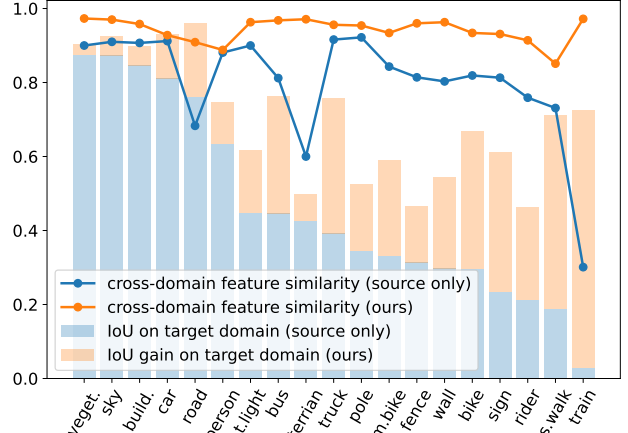


Figure 2. **Category-wise cross-domain feature similarity as well as the evaluation results on the target domain.** When directly testing the model trained with source data (*i.e.*, “source only”) on the target data, the categories, where source and target features are *largely dissimilar* to each other, suffer from low IoU. We substantially improve the performance by *pulling close* per-category features from these two domains.

on Cityscapes, we improve the baseline by +2.5% and +2.1%, respectively.

2. Related Work

Unsupervised domain adaptive semantic segmentation aims at learning a generalized segmentation model that can adapt from a labeled (synthetic) source domain to an unlabeled (real-world) target domain. To overcome the domain gap, most previous methods align distributions of source and target domains to an *intermediate common space* at the image level [20, 48, 60, 37], feature level [21, 22, 20, 59, 3, 4], and output level [65, 44] by introducing extra objectives or techniques, *e.g.*, optimizing some custom distance [40, 30], applying computationally adversarial training [17, 49, 65, 44, 7, 66], offline pseudo-labeling [84, 37, 85], and image translation models [20, 37]. Different from these methods, as illustrated in Fig. 1b, based on the observation that source features are always capable during training, we *pull target features close to source features for each category*. Through this way, T2S-DA manages to learn similar cross-domain features for each category. Shown in Fig. 2, the improved cross-domain feature similarity indeed boosts the segmentation results. One may concern that making source close to target seems to be a reasonable alternative. We compare this strategy, *i.e.*, “source \rightarrow target”, to our T2S-DA in Sec. 4.2, where we empirically find that this explicit alignment works *only when pulling target to source*.

Domain generalized semantic segmentation is a more challenging task compared to domain adaptation. It assumes target data is unaccessible during training, focusing on gen-

eralizing well on *unseen* target domains. To extract domain-invariant feature representations, plenty of approaches have been proposed such as meta-learning [31, 2, 32, 36], adversarial training [33, 35, 55], metric-learning [47, 13], and feature normalization [53, 25, 8]. Few attempts have been made in domain generalization based on cross-domain alignment. Our T2S-DA is proved to be efficient for both settings, verifying that similar cross-domain features do contribute to better segmentation results.

3. Method

In this section, we formulate the UDA problem and present an overview of our proposed T2S-DA in Sec. 3.1. In Sec. 3.2, we explain how to pull target to source with different objectives, including InfoNCE and MSE. Two sample strategies are introduced in Sec. 3.3. Finally, in Sec. 3.4, we describe the dynamic re-weighting strategy to make the model focus on underperforming categories.

3.1. Overview

Unsupervised domain adaptive semantic segmentation aims at applying a model learned from the labeled source dataset $\mathcal{D}_s = \{(\mathbf{x}_i^s, \mathbf{y}_i^s)\}_{i=1}^{n_s}$ to the unlabeled target dataset $\mathcal{D}_t = \{\mathbf{x}_i^t\}_{i=1}^{n_t}$, where n_s and n_t are the numbers of images of source and target domains, respectively. $\mathbf{x}_i^s \in \mathbb{R}^{H \times W \times 3}$ and $\mathbf{x}_i^t \in \mathbb{R}^{H \times W \times 3}$ are RGB images, while $\mathbf{y}_i^s \in \mathbb{R}^{H \times W \times C}$ is the one-hot semantic map associated with \mathbf{x}_i^s . Source and target datasets share the same label space with C categories. Following previous methods [23, 78, 34, 14, 69], we adopt self-training as the baseline, where source data are used under a supervised manner and the unsupervised loss is computed based on target images and their pseudo-labels generated by a momentum teacher. Concretely, our proposed T2S-DA follows the Mean Teacher [63] framework that consists of a student and a teacher. Each model ψ reparameterized by θ consists of an encoder $h : \mathbb{R}^{H \times W \times 3} \rightarrow \mathbb{R}^{h \times w \times D}$ followed by a segmentor $f : \mathbb{R}^{h \times w \times D} \rightarrow (0, 1)^{H \times W \times C}$ and a projector $g : \mathbb{R}^{h \times w \times D} \rightarrow \mathbb{R}^{h \times w \times d}$, where H and W indicate the height and width of the input image respectively. h , w and D form the shape of the intermediate features, and d is the feature dimension of the projector. The teacher is momentum updated by the student, *i.e.*, $\theta_t \leftarrow \eta\theta_t + (1 - \eta)\theta_s$, where η is a momentum coefficient. θ_s and θ_t are parameters of the student ψ_s and the teacher ψ_t , respectively.

The overall objective is the sum of source supervised loss, target unsupervised loss, and pulling loss: $\mathcal{L} = \mathcal{L}_{\text{source}} + \mathcal{L}_{\text{target}} + \lambda\mathcal{L}_{\text{pull}}$. For source data, we naively train the student with categorical cross-entropy (CE)

$$\mathcal{L}_{\text{source}} = \sum_{i=1}^{n_s} \sum_{j=1}^{H \times W} \ell_{ce} [f_s(h_s(\mathbf{x}_i^s))(j), \mathbf{y}_i^s(j)], \quad (1)$$

where $\ell_{ce}(\mathbf{p}, \mathbf{y}) = -\mathbf{y}^\top \log \mathbf{p}$. For unlabeled target data, we minimize the weighted cross-entropy loss between predictions and pseudo-labels $\hat{\mathbf{y}}^t$ generated by the teacher, where $\hat{\mathbf{y}}_i^t(j) = \text{one_hot}[\arg \max_c f_t(h_t(\mathbf{x}_i^t))(j, c)]$. Details can be found in *Supplementary Material*.

As discussed in Sec. 1, we observe that the model trained with source data is able to build a capable source feature space, but when we apply it to target domain, the features run into undesirable chaos. *The performance drop is highly related to the cross-domain feature dissimilarity* caused by the domain gap. Intuitively, if we pull target features to source ones, it implicitly implies an adequate feature space for segmenting target samples. To this end, we aim to conduct *cross-domain positive pairs*, *i.e.*, $(\mathbf{q}, \mathbf{k}^+)$, from the *exactly* same category but different domains, and then maximize their agreement. We study two objectives for this procedure, including InfoNCE [51] and MSE.

InfoNCE [51] pulls together positive pairs $(\mathbf{q}, \mathbf{k}^+)$ and pushes away negative pairs $(\mathbf{q}, \mathbf{k}^-)$.

$$\mathcal{L}_{\text{InfoNCE}}(\mathbf{q}, \mathbf{k}^+) = -\log \left[\frac{e^{(\mathbf{q}^\top \mathbf{k}^+ / \tau)}}{e^{(\mathbf{q}^\top \mathbf{k}^+ / \tau)} + \sum_{\mathbf{k}^- \in \mathcal{K}_{\mathbf{q}}^-} e^{(\mathbf{q}^\top \mathbf{k}^- / \tau)}} \right], \quad (2)$$

where \mathbf{q} , \mathbf{k}^+ and \mathbf{k}^- are ℓ_2 -normalized features, which are outputs of the projector. τ indicates the temperature. $\mathcal{K}_{\mathbf{q}}^-$ is the set of negative keys of the given query \mathbf{q} , which is introduced in Sec. 3.2.

$\mathcal{L}_{\text{MSE}}(\mathbf{q}, \mathbf{k}^+) = \|\mathbf{q} - \mathbf{k}^+\|_2^2$, which maximizes the similarity of positive pairs $(\mathbf{q}, \mathbf{k}^+)$ directly.

The pulling objective is *weighted* over each positive pair

$$\mathcal{L}_{\text{pull}} = \frac{1}{C} \sum_{c=0}^{C-1} w_c^* \sum_{(\mathbf{q}, \mathbf{k}^+) \in \mathcal{K}_c^+} \mathcal{L}_{\text{pull}}(\mathbf{q}, \mathbf{k}^+), \quad (3)$$

where \mathcal{K}_c^+ indicates the set of positive keys for category c described later in Sec. 3.2. w_c^* is the weight of class c , which is dynamically adjusted and discussed in Sec. 3.4. $\mathcal{L}_{\text{pull}}(\mathbf{q}, \mathbf{k}^+)$ is the pulling loss given a pair of positive features, which is either MSE or InfoNCE [51].

3.2. Pulling Target to Source

In this section, we describe how to generate positive pairs that *exactly* belong to the same category without target annotations. Next, we take $\mathcal{L}_{\text{InfoNCE}}$ as the alignment objective, and provide detailed formulations.

We employ an image translation engine to make sure cross-domain positive pairs belong to the same category. Illustrated in Fig. 3, we first feed source data \mathbf{x}^s into the image translation engine \mathcal{T} (FDA [77] in this paper) to produce *pseudo-target* data $\mathcal{T}(\mathbf{x}^s)$, which naturally have annotations, and then urge the model to learn similar features

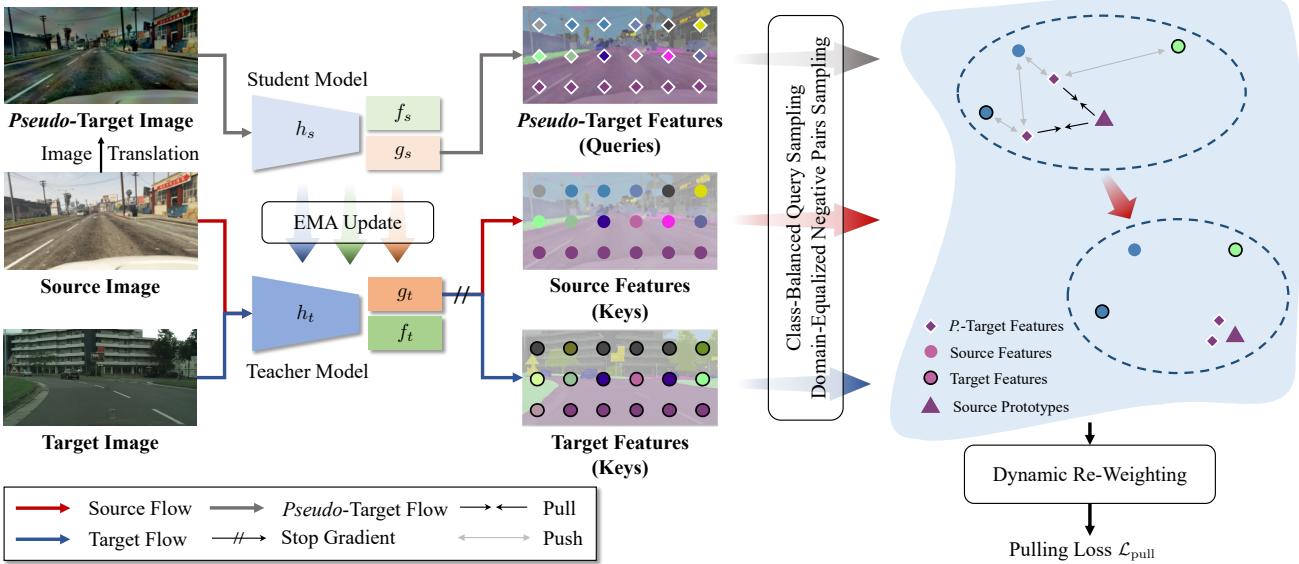


Figure 3. **Illustration of contrastive pairs.** We regard features from *pseudo-targets* and *source prototypes* of the same category as the positive pairs defined in Eq. (5). Negative keys include 1) source features from a different category (as in Eq. (7)), and 2) unreliable target features from a different category (as in Eq. (8)). In this way, this model is encouraged to *learn similar features between the source and target domains from any category*. The improved similarity indeed boosts segmentation results (see Fig. 2).

across source and pseudo-target domains regarding each category, *i.e.*, pulling features of $\mathcal{T}(\mathbf{x}^s)$ close to features of \mathbf{x}^s for each class. Formulations are provided as follows.

Queries \mathbf{q} are features to be optimized, and thus they come from pseudo-target images $\mathcal{T}(\mathbf{x}^s)$

$$\mathcal{Q}_c = \{g_s(h_s(\mathcal{T}(\mathbf{x}^s)))(j) \mid y^s(j, c) = 1\}, \quad (4)$$

where $j = 1, 2, \dots, h \times w$ is the pixel index, and we randomly sample $n_q(c)$ queries for class c at each iteration, which will be discussed later in Sec. 3.3.

Positive pairs $(\mathbf{q}, \mathbf{k}^+)$ are the crux for T2S-DA. To learn similar cross-domain features, their agreements are supposed to be maximized. Given a query $\mathbf{q} \in \mathcal{Q}_c$ belongs to class c , its positive key \mathbf{k}^+ is defined as the *source prototype* of class c generated by the momentum teacher. Concretely, given an mini-batch $\mathcal{B} = (\mathbf{x}^s, \mathbf{y}^s, \mathbf{x}^t)$, we compute the source prototype of class c by

$$\mathbf{k}_c^+ = \frac{\sum_{j=1}^{h \times w} \mathbb{1}[y^s(j, c) = 1] \cdot [g_t(h_t(\mathbf{x}^s))(j)]}{\sum_{j=1}^{h \times w} \mathbb{1}[y^s(j, c) = 1]}. \quad (5)$$

Therefore, the set of positive pairs is defined as

$$\mathcal{K}^+ = \bigcup_{c=0}^{C-1} \{(\text{norm}(\mathbf{q}), \text{norm}(\mathbf{k}_c^+)) \mid \mathbf{q} \in \mathcal{Q}_c\}, \quad (6)$$

where $\text{norm}(\cdot)$ represents the ℓ_2 -norm, and \mathcal{Q}_c is the set of candidate queries defined in Eq. (4). Thanks to the image translation engine, we manage to conduct \mathbf{q} and \mathbf{k}^+ that belong to the *exact* category even without target labels.

Negative pairs $(\mathbf{q}, \mathbf{k}^-)$ are used to avoid model collapse [18, 6] in InfoNCE [51], which is not out main focus. Given a query $\mathbf{q} \in \mathcal{Q}_c$ belongs to class c , its negative keys consist of features from both domains. For source features, we simply choose features that do not belong to category c

$$\mathcal{K}_s^-(c) = \{g_t(h_t(\mathbf{x}^s))(j) \mid y^s(j, c) = 0\}, \quad (7)$$

where $j = 1, 2, \dots, h \times w$ denotes the pixel index. The subscript s here stands for “source”. For target features, inspired by [72], we take those unreliable features into consideration, fully mining the inherit information behind target domain. Specifically, we regard features 1) whose confidence are in the last α percent and 2) are predicted not to belong to category c as candidate negative samples

$$\mathcal{K}_t^-(c) = \{g_t(h_t(\mathbf{x}^t))(j) \mid \max_{c'} f_t(h_t(\mathbf{x}^t))(j, c') < \gamma, \hat{y}^t(j, c) = 0\}, \quad (8)$$

where $\max_{c'} f_t(h_t(\mathbf{x}^t))(j, c')$ indicates the confidence (*i.e.*, maximum probability) of target image \mathbf{x}^t at pixel j . The subscript t here stands for “target”. γ is the confidence threshold related to unreliable partition α , satisfying

$$\sum_{j=1}^{h \times w} \mathbb{1}[\max_{c'} f_t(h_t(\mathbf{x}^t))(j, c') < \gamma] = \alpha \cdot (h \cdot w), \quad (9)$$

i.e., $\gamma = \text{np.percentile}(\mathbf{C}.\text{flatten}(), 100 \cdot \alpha)$, and \mathbf{C} is the confidence matrix. Overall, the set of negative

keys for query \mathbf{q} is:

$$\mathcal{K}_{\mathbf{q}}^- = \bigcup_{c=0}^{C-1} \{\text{norm}(\mathbf{k}_c^-) \mid \mathbf{k}_c^- \in \mathcal{K}_s^-(c) \cup \mathcal{K}_t^-(c)\}. \quad (10)$$

Discussion. T2S-DA tries to make target features (usually noisy) close to source features without target annotations. Therefore, we regard pseudo-target features as queries and try to make them similar to *consistent* positive keys (*i.e.*, source features extracted by the momentum teacher).

3.3. Sampling Strategies

Class-balanced query sampling. Semantic segmentation usually suffers from a long-tailed label distribution. To alleviate this issue, a vanilla method is class-equalized query sampling (CEQS), treating all categories equally, *i.e.*, the number of queries $n_q(c)$ of class c equals to n for each c . However, CEQS tends to oversample rare classes whose features are usually noisy and unstable, leading to extra training noise. To this end, we adopt class-balanced query sampling (CBQS) based on the label distribution of the current mini-batch. Specifically, given an input mini-batch $\mathcal{B} = (\mathbf{x}^s, \mathbf{y}^s, \mathbf{x}^t)$, we first compute the distribution of \mathbf{y}^s

$$\hat{p}(c) = \frac{\sum_{j=1}^{h \times w} \mathbb{1}[y^s(j, c) = 1]}{\sum_{c=0}^{C-1} \sum_{j=1}^{h \times w} \mathbb{1}[y^s(j, c) = 1]}. \quad (11)$$

Next, based on \hat{p} and the base sample number n , we define $n_q(c) = \lceil C \cdot \hat{p}(c) \cdot n \rceil$.

Domain-equalized negative pair sampling. After we get the set of candidate negative pairs, a straightforward solution is to sample m negative pairs from \mathcal{K}^- directly. However, the proportion of negative samples from each domain (*i.e.*, source and target domains) can be unstable under such a strategy. The more samples from \mathcal{K}_s^- are introduced, the more homogeneous for all negative pairs. By contrast, the more samples from \mathcal{K}_t^- are applied, the more unstable training procedure we have due to the *false negative* issue owing to the lack of target ground-truths. Therefore, to balance the stability during training (by introducing more $\mathbf{k}^- \in \mathcal{K}_s^-$) and the enrichment of negative samples (by introducing more $\mathbf{k}^- \in \mathcal{K}_t^-$), we adopt domain-equalized negative pair sampling (DENPS), where we randomly sample $m/2$ features from \mathcal{K}_s^- and $m/2$ features from \mathcal{K}_t^- .

3.4. Dynamic Re-Weighting

Due to the limited labeled source data and the existing domain shift, the training tends to be biased to dominant categories [84, 85]. To address this, we propose a novel dynamic re-weighting strategy which urges the model paying more attention on underperforming classes and prevents it from being overwhelmed by well-trained samples.

Concretely, for class c , we define its weight w_c^* in the pulling loss as $w_c^* = w_c / \left(\sum_{c=0}^{C-1} w_c \right)$, where w_c is the weight computed based on the mean confidence

$$w_c = \left[\frac{1 - \text{conf}(c)}{\max_{c'} (1 - \text{conf}(c'))} \right]^\beta, \quad (12)$$

where $\beta = 0.5$ is a scale factor and $\text{conf}(c)$ denotes the mean confidence (*i.e.*, maximum probability) of class c on target in current mini-batch $\mathcal{B} = (\mathbf{x}^s, \mathbf{y}^s, \mathbf{x}^t)$, which can be jointly calculated by pseudo-labels $\hat{\mathbf{y}}^t$ and teacher predictions $f_t(h_t(\mathbf{x}^t))$

$$\text{conf}(c) = \frac{\sum_{j=1}^{H \times W} \mathbb{1}[\hat{y}^t(j, c) = 1] \cdot [\max_{c'} f_t(h_t(\mathbf{x}^t))(j, c')]}{\sum_{j=1}^{H \times W} \mathbb{1}[\hat{y}^t(j, c) = 1]}. \quad (13)$$

4. Experiments

Datasets. We regard GTA5 [56] and SYNTHIA [58] as source domain, and Cityscapes [11] as target domain. GTA5 [56] contains 24, 966 synthetic images with resolution 1914×1052 , and SYNTHIA [58] consists of 9, 400 synthetic images with resolution 1280×760 . As for the target Cityscapes [11], it has 2, 975 training and 500 validation images with resolution 2048×1024 .

Training. We first resize target images to 1024×512 and source images from GTA5 [56] to 1280×720 . Then, we random crop source images to 1024×512 and adopt FDA [77] to build the pseudo-target domain. Finally, we randomly crop them into 512×512 for further training. We adopt AdamW [42] with betas $(0.9, 0.999)$, a learning rate of 6×10^{-5} for the encoder and 6×10^{-4} for the segmentor and the projector, a weight-decay of 0.01, linear learning rate warmup schedule with $t_{\text{warm}} = 1.5k$. The model is trained with a batch of two source images and two target images, for 40k iterations. In accordance with [64], we set $\eta = 0.999$. Temperature $\tau = 0.2$, scale factor $\beta = 0.5$, unreliable partition $\alpha = 50\%$, base number of queries $n = 128$, number of negative pairs per query $m = 1024$. All experiments are conducted on 1 Tesla A100 GPU based on PyTorch [54] and mmsegmentation [10].

Network architecture. Start from using the DeepLab-V2 [5] as the segmentor f with ResNet-101 [19] as the encoder h , we adopt DACS [64] with two extra strategies in [23] as baseline. To further verify the efficiency of T2S-DA on recent Transformer-based networks, we use DAFormer [23] as a stronger baseline, where h is the MiT-B5 encoder [75] and f is the DAFormer decoder [23]. The projector g takes the feature provided by the encoder (2, 048-dimensional for ResNet-101 [19] and 512-dimensional for MiT-B5 [75]) as input, and consists of two Conv-BN-ReLU blocks, where both blocks preserve the feature map resolution and map the number of channels to 256.

Table 1. Comparison with state-of-the-art alternatives on **GTA5 → Cityscapes** benchmark. The results are averaged over 3 random seeds. The top performance is highlighted in **bold** font. \dagger means we reproduce the approach.

Method	Road	S.walk	Build.	Wall	Fence	Pole	T.light	Sign	Veget.	Terrain	Sky	Person	Rider	Car	Truck	Bus	Train	M.bike	Bike	mIoU
<i>CNN-based</i>																				DeepLab-V2 [5] with ResNet-101 [19]
source only \dagger	70.2	14.6	71.3	24.1	15.3	25.5	32.1	13.5	82.9	25.1	78.0	56.2	33.3	76.3	26.6	29.8	12.3	28.5	18.0	38.6
FDA [77]	92.5	53.3	82.4	26.5	27.6	36.4	40.6	38.9	82.3	39.8	78.0	62.6	34.4	84.9	34.1	53.1	16.9	27.7	46.4	50.5
ProDA [78]	91.5	52.4	82.9	42.0	35.7	40.0	44.4	43.3	87.0	43.8	79.5	66.5	31.4	86.7	41.1	52.5	0.0	45.4	53.8	53.7
T2S-DA (ours)	96.2	73.4	88.6	45.1	37.4	40.7	54.0	55.5	88.9	48.6	88.2	72.2	45.0	89.6	53.8	56.2	1.3	53.0	59.6	60.4
<i>Transformer-based</i>																				DAFormer [23] with MiT-B5 [75]
source only \dagger	76.1	18.7	84.6	29.8	31.4	34.5	44.8	23.4	87.5	42.6	87.3	63.4	21.2	81.1	39.3	44.6	2.9	33.2	29.7	46.1
DAFormer [23]	95.7	70.2	89.4	53.5	48.1	49.6	55.8	59.4	89.9	47.9	92.5	72.2	44.7	92.3	74.5	78.2	65.1	55.9	61.8	68.3
DAFormer (w/ FDA) \dagger	95.4	68.2	89.8	52.9	45.1	51.4	60.9	51.2	90.1	48.6	92.6	75.0	45.9	93.0	72.4	74.3	62.1	62.3	66.3	68.8
FST [14]	95.3	67.7	89.3	55.5	47.1	50.1	57.2	58.6	89.9	51.0	92.9	72.7	46.3	92.5	78.0	81.6	74.4	57.7	62.6	69.3
T2S-DA (ours)	95.9	71.1	89.9	54.5	46.6	52.4	61.6	61.0	90.3	49.8	92.5	74.6	46.3	93.2	75.8	76.3	72.4	58.9	66.8	70.0
HRDA [24]	96.4	74.4	91.0	61.6	51.5	57.1	63.9	69.3	91.3	48.4	94.2	79.0	52.9	93.9	84.1	85.7	75.9	63.9	67.5	73.8
T2S-DA (ours)	96.8	76.2	90.8	67.3	56.1	59.7	64.3	68.9	90.7	53.0	92.5	78.3	56.1	93.7	81.8	86.3	76.2	67.3	70.1	75.1

Table 2. Comparison with state-of-the-art alternatives on **SYNTHIA → Cityscapes** benchmark. The results are averaged over 3 random seeds. The mIoU and the mIoU* indicate we compute mean IoU over 16 and 13 categories, respectively. The top performance is highlighted in **bold** font. \dagger means we reproduce the approach.

Method	Road	S.walk	Build.	Wall*	Fence*	Pole*	T.light	Sign	Veget.	Sky	Person	Rider	Car	Bus	M.bike	Bike	mIoU	mIoU*	
<i>CNN-based</i>																			DeepLab-V2 [5] with ResNet-101 [19]
source only \dagger	55.6	23.8	74.6	9.2	0.2	24.4	6.1	12.1	74.8	79.0	55.3	19.1	39.6	23.3	13.7	25.0	33.5	38.6	
FDA [77]	79.3	35.0	73.2	-	-	-	19.9	24.0	61.7	82.6	61.4	31.1	83.9	40.8	38.4	51.1	-	52.5	
ProDA [78]	87.1	44.0	83.2	26.9	0.7	42.0	45.8	34.2	86.7	81.3	68.4	22.1	87.7	50.0	31.4	38.6	51.9	58.5	
T2S-DA (ours)	81.2	38.3	86.0	26.5	1.8	43.8	48.0	54.6	85.2	86.6	73.0	40.8	87.5	52.8	52.2	62.6	57.6	65.4	
<i>Transformer-based</i>																			DAFormer [23] with MiT-B5 [75]
source only \dagger	56.5	23.3	81.3	16.0	1.3	41.0	30.0	24.1	82.4	82.5	62.3	23.8	77.7	38.1	15.0	23.7	42.4	47.7	
DAFormer [23]	84.5	40.7	88.4	41.5	6.5	50.0	55.0	54.6	86.0	89.8	73.2	48.2	87.2	53.2	53.9	61.7	60.9	67.4	
DAFormer (w/ FDA) \dagger	76.9	32.6	88.2	41.1	5.2	54.1	61.3	55.7	87.1	90.0	76.8	48.7	87.8	55.4	57.2	63.7	61.4	67.8	
FST [14]	88.3	46.1	88.0	41.7	7.3	50.1	53.6	52.5	87.4	91.5	73.9	48.1	85.3	58.6	55.9	63.4	61.9	68.6	
T2S-DA (ours)	87.6	46.0	88.8	43.7	6.4	53.3	59.1	54.8	87.5	91.1	75.7	47.6	88.2	58.0	54.9	62.4	62.8	69.4	
HRDA [24]	85.2	47.7	88.8	49.5	4.8	57.2	65.7	60.9	85.3	92.9	79.4	52.8	89.0	64.7	63.9	64.9	65.8	72.4	
T2S-DA (ours)	85.7	50.3	88.5	50.1	9.7	61.7	67.1	62.3	84.7	93.0	77.9	56.1	89.3	68.2	65.7	70.3	67.5	73.8	

4.1. Comparison with Existing Alternatives

From Tabs. 1 and 2, we can tell that by making the model learn similar features across domains, T2S-DA outperforms state-of-the-art competitors on various benchmarks. Note that, we report the performances of ProDA [78] without knowledge distillation using self-supervised pretrained models for a fair comparison. Specifically, with CNN-based [29] network, T2S-DA surpasses ProDA [78] by +6.7% mIoU on GTA5 → Cityscapes, +5.7% mIoU on SYNTIA → Cityscapes (16 classes), and +6.9% mIoU* on SYNTIA → Cityscapes (13 classes), respectively. With Transformer-based [12] network, T2S-DA surpasses DAFormer [23] by +1.7% mIoU on GTA5 → Cityscapes, +1.9% mIoU on SYNTIA → Cityscapes (16 classes), and +2.0% mIoU* on SYNTIA → Cityscapes (13 classes), respectively. Specifically, benefiting from learning similar features across

domains, T2S-DA improves the performances of class “sidewalk” by +21.0% compared to ProDA [78] and class “train” by +10.3% compared to DAFormer [23] on GTA5 → Cityscapes benchmark. On SYNTIA → Cityscapes, T2S-DA outperforms FDA [77] on class “motorbike” by +13.8% and surpasses ProDA [78] on class “sign” by +20.4%. Note that FST [14] requires 4× training time by default. Extended comparison can be found in *Supplementary Material*.

Qualitative results. Fig. 4 gives visualization results of different methods evaluated on GTA5 → Cityscapes benchmark. We compare the proposed T2S-DA with ground truths and a strong baseline DAFormer [23]. Benefiting from a series of technologies designed for building the category-discriminative target feature representation space, T2S-DA achieves great performance on difficult categories. More results can be found in *Supplementary Material*.

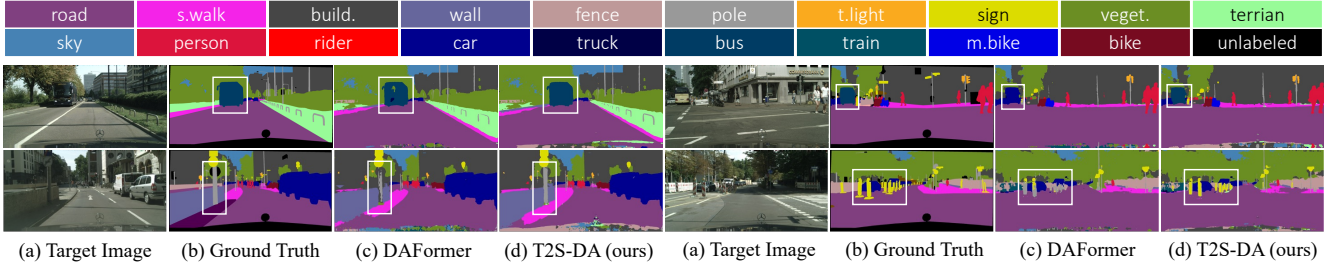


Figure 4. **Qualitative comparison**, where white rectangles highlight the visual improvements (best-viewed zoomed-in). From left to right: target image, ground truth, the segmentation maps predicted by our baseline DAFormer [23] and our T2S-DA, are shown one by one.

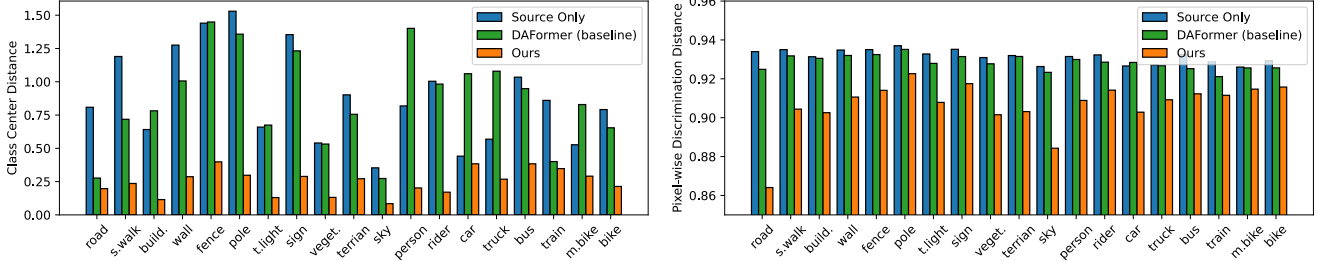


Figure 5. **Analysis of the feature discriminativeness**. For each class, we show the values of class center distance [68] and pixel-wise discrimination distance [74] on Cityscapes val set. For both metrics, a *smaller* value indicates *stronger* discrimination.

4.2. Ablation Studies

All ablations in this section are conducted on the GTA5 \rightarrow Cityscapes benchmark with Transformer-based architecture.

Effectiveness of pulling target to source. We take DAFormer [23] as our baseline. Simply apply FDA [77] to DAFormer [23], *i.e.*, compute the supervised loss defined in Eq. (1) on the pseudo-target domain, brings little improvements. Vanilla contrast on the source domain also brings neglectable improvements. When simply pulling source close to target, the performance maintains 68.3% but with a larger standard deviation of 1.1%. This is because, without target labels, it is hard to conduct positive pairs precisely. To this end, we introduce an image translation engine to ensure true positive matches, but the improvements still remain limited, *i.e.*, 69.0%. However, when changing the direction of this alignment, *i.e.*, *pulling target to source*, however, the performance achieves 70.0%, bringing an improvement of +1.7%. In addition, if we compute cross-entropy on the pseudo target domain on the basis of T2S-DA, the performance drops to 69.0%. In conclusion, the alignment works *only when we pull target to source*.

case	CE	q	k^+	mIoU
DAFormer [23]	source	-	-	68.3 \pm 0.5
DAFormer (w/ FDA)	p. target	-	-	68.8 \pm 0.8
vanilla contrast	source	source	source	68.5 \pm 0.3
source \rightarrow target	source	source	target	68.3 \pm 1.1
source \rightarrow p. target	source	source	p. target	69.0 \pm 0.3
T2S-DA	source	p. target	source	70.0 \pm 0.6
p. target \rightarrow source	p. target	p. target	source	69.0 \pm 1.6

Effectiveness of different objectives. InfoNCE is the default alignment objective by default, however, *our mo-*

tivation is not limited to contrastive learning. Interestingly, when replacing the InfoNCE with the MSE loss between ℓ_2 -normalized positive pairs (q, k^+), it can still boost the performance with +2.3% and +1.1% mIoU improvements using CNN-based models and Transformer-based models, respectively. Details can be found in the following table.

encoder	decoder	alignment	mIoU
ResNet-101 [19]	DeepLab-V2 [5]	none	56.3
ResNet-101 [19]	DeepLab-V2 [5]	MSE	58.6 \uparrow 2.3
ResNet-101 [19]	DeepLab-V2 [5]	InfoNCE	60.4 \uparrow 4.1
MiT-B5 [75]	DAFormer [23]	none	68.3
MiT-B5 [75]	DAFormer [23]	MSE	69.4 \uparrow 1.1
MiT-B5 [75]	DAFormer [23]	InfoNCE	70.0 \uparrow 1.7

Effectiveness of sample strategies. We study the effectiveness of our proposed sampling strategies introduced in Sec. 3.3, *i.e.*, class-balanced query sampling (CBQS), and domain-equalized negative pair sampling (DENPS), in the right table. Notably, only when combined these two strategies together, brings significant improvements. On one hand, without CBQS, queries are easily overwhelmed by those dominant classes, *e.g.*, road and sky. On the other hand, without DENPS, the model tends to neglect target features in contrastive learning.

	DRW	mIoU	mIoU (Tail)
none	68.9 \pm 0.6	62.0 \pm 1.1	
$\mathcal{L}_{\text{target}}$	68.8 \pm 0.4 \downarrow 0.1	60.1 \pm 1.3 \downarrow 1.8	
$\mathcal{L}_{\text{pull}}$	70.0 \pm 0.6 \uparrow 1.1	63.7 \pm 0.8 \uparrow 1.7	

Applying DRW to $\mathcal{L}_{\text{target}}$ rather than $\mathcal{L}_{\text{pull}}$ can be an

Table 3. Effectiveness of our T2S-DA on **domain generalized semantic segmentation**. (G) indicates the model is trained on GTA5 and evaluated on Cityscapes, and (S) denotes the SYNTHIA counterpart. Note that for (S) methods, we compute mean IoU over 16 classes for comparison. The top performance is highlighted in **bold** font. All results are averaged over 3 different random seeds.

Method	Road	S.walk	Build.	Wall	Fence	Pole	Light	Sign	Veget.	Terrain	Sky	Person	Rider	Car	Truck	Bus	Train	M.bike	Bike	mIoU
Baseline (G)	76.1	18.7	84.6	29.8	31.4	34.5	44.8	23.4	87.5	42.6	87.3	63.4	21.2	81.1	39.3	44.6	2.9	33.2	29.7	46.1±1.2
T2S-DA (G, ours)	80.7	27.9	85.9	35.2	31.9	36.6	45.1	30.6	87.6	44.5	87.6	64.3	24.4	88.5	42.8	41.0	12.0	30.8	26.3	48.6 ±1.2
Baseline (S)	56.5	23.3	81.3	16.0	1.3	41.0	30.0	24.1	82.4	-	82.5	62.3	23.8	77.7	-	38.1	-	15.0	23.7	42.4±1.9
T2S-DA (S, ours)	68.0	27.0	82.2	20.5	1.7	42.3	33.4	28.2	81.8	-	84.0	60.6	24.1	75.1	-	38.9	-	16.6	26.8	44.5 ±1.1

alternative. However, as underperforming categories tend to suffer from greater domain shifts, their target pseudo-labels can be noisy. It is risky to optimize those classes using the cross-entropy loss directly. To this end, it is better to combine DRW with $\mathcal{L}_{\text{pull}}$, urging the model put more effort into learning similar cross-domain features for these categories. From the table, we can tell that *only when DRW is equipped with $\mathcal{L}_{\text{pull}}$, it brings significant improvements, especially in tailed classes*. Per-class performances can be found in *Supplementary Material*.

Effectiveness of the image translation engine. We conduct experiments in the right table to verify the effectiveness of different image translation engines. Implementation details of ColorJitter and GaussianBlur are the same with SimCLR [6]. We adopt FDA [77] simply because it does not need extra training. This empirical evidence demonstrates that in our T2S-DA, it is not necessary to exactly *fit* the target domain. In other words, T2S-DA learns domain-invariant features *no matter what kind of transformation is adopted*.

4.3. Discriminativeness Analysis

To verify whether our T2S-DA has indeed built a more discriminative target representation space compared with previous alternatives, we adopt metrics used in FADA [68] and SePiCo [74] to take a closer look at what degree the representations are aligned at category-level and pixel-level, respectively. We compare the discrimination of target feature space between (1) the source only baseline, (2) DAFormer [23], and (3) our T2S-DA. We calculate these metrics on the whole Cityscapes [11] validation set. Detailed formulations of these two metrics are given below.

Class center distance (CCD) is the ratio of intra-class compactness over inter-class distance [68]

$$CDD(i) = \frac{1}{C-1} \sum_{j=0, j \neq i}^{C-1} \frac{\frac{1}{|\Omega_i|} \sum_{\mathbf{x} \in \Omega_i} \|\mathbf{x} - \boldsymbol{\mu}_i\|^2}{\|\boldsymbol{\mu}_i - \boldsymbol{\mu}_j\|^2}, \quad (14)$$

where $\boldsymbol{\mu}_i$ is the prototype or center of category i and Ω_i is the set of features that belong to class i .

Pixel-wise discrimination distance (PDD) is to evaluate the effectiveness of pixel-wise representation alignment [74]. We modify it into 1 minus its original value for a more straightforward comparison together with CCD.

$$PDD(i) = 1 - \frac{1}{|\Omega_i|} \sum_{\mathbf{x} \in \Omega_i} \frac{\cos(\mathbf{x}, \boldsymbol{\mu}_i)}{\sum_{j=0, j \neq i}^{C-1} \cos(\mathbf{x}, \boldsymbol{\mu}_j)}. \quad (15)$$

Low CCD and PDD suggest the features of the same class have been densely clustered while the distances between different categories are relatively large at category-level and pixel-level, respectively. We compare CCD and PDD values with source only model and DAFormer [23]. As illustrated in Fig. 5, T2S-DA achieves much smaller CCD and PDD values in each category compared with others. This empirical evidence verifies that by pulling target features close to source ones for each category, T2S-DA indeed learns a more discriminative target feature space, resulting in better segmentation performances.

4.4. Domain Generalized Semantic Segmentation

We further evaluate our proposed T2S-DA on domain generalized (DG) semantic segmentation, where images from the target domain are unaccessible, making it more important to extract domain-invariant feature representations [8]. We adopt the translation model provided by Kundu *et al.* [27] rather than FDA [77], since it does not require access to target images. Note that we cannot apply $\mathcal{L}_{\text{target}}$, dynamic re-weighting, and domain-equalized negative pair sampling since we fail to get target samples in DG, and thus the overall objective becomes $\mathcal{L}_{\text{source}} + \lambda \mathcal{L}_{\text{pull}}$.

We take DAFormer [23] trained with only source images in a fully-supervised manner as the baseline. As illustrated in Tab. 3, T2S-DA manages to bring significant improvements over baseline, verifying its domain-invariant property.

5. Conclusion

In this paper, we present T2S-DA, which is able to build a category-discriminative target feature space via *pulling target close to source*, leading to better segmentation results. Experimental results show significant growths, and T2S-DA proves to be very efficient at avoiding models being

trapped in domain-specific styles, outperforming state-of-the-art alternatives on various UDA benchmarks. Moreover, it can be applied to DG thanks to its domain-invariant property.

Discussion. As discussed in [77], image translation models are unstable, although it is better than using target pseudo-labels directly. Therefore, how to conduct positive pairs to alleviate the false positive issue without introducing extra noise could be further studied. Additionally, as the entire real world is the target domain in domain generalization, how to conduct a pseudo-target that is able to *almost* cover the target remains an open problem.

References

- [1] Nikita Araslanov and Stefan Roth. Self-supervised augmentation consistency for adapting semantic segmentation. In *Proceedings of the IEEE/CVF Conference on Computer Vision and Pattern Recognition (CVPR)*, 2021. **1, 2, 12, 13**
- [2] Yogesh Balaji, Swami Sankaranarayanan, and Rama Chellappa. Metareg: Towards domain generalization using meta-regularization. *Advances in Neural Information Processing Systems (NeurIPS)*, 2018. **3**
- [3] Wei-Lun Chang, Hui-Po Wang, Wen-Hsiao Peng, and Wei-Chen Chiu. All about structure: Adapting structural information across domains for boosting semantic segmentation. In *Proceedings of the IEEE/CVF Conference on Computer Vision and Pattern Recognition (CVPR)*, 2019. **2**
- [4] Chaoqi Chen, Weiping Xie, Wenbing Huang, Yu Rong, Xinghao Ding, Yue Huang, Tingyang Xu, and Junzhou Huang. Progressive feature alignment for unsupervised domain adaptation. In *Proceedings of the IEEE/CVF Conference on Computer Vision and Pattern Recognition (CVPR)*, 2019. **2**
- [5] Liang-Chieh Chen, George Papandreou, Iasonas Kokkinos, Kevin Murphy, and Alan L Yuille. Deeplab: Semantic image segmentation with deep convolutional nets, atrous convolution, and fully connected crfs. *IEEE Transactions on Pattern Analysis and Machine Intelligence (TPAMI)*, 2017. **5, 6, 7, 12, 13, 15**
- [6] Ting Chen, Simon Kornblith, Mohammad Norouzi, and Geoffrey Hinton. A simple framework for contrastive learning of visual representations. In *International Conference on Machine Learning (ICML)*, 2020. **4, 8**
- [7] Yuhua Chen, Wen Li, Xiaoran Chen, and Luc Van Gool. Learning semantic segmentation from synthetic data: A geometrically guided input-output adaptation approach. In *Proceedings of the IEEE/CVF Conference on Computer Vision and Pattern Recognition (CVPR)*, 2019. **2**
- [8] Sungha Choi, Sanghun Jung, Huiwon Yun, Joanne T Kim, Seunghyong Kim, and Jaegul Choo. Robustnet: Improving domain generalization in urban-scene segmentation via instance selective whitening. In *Proceedings of the IEEE/CVF Conference on Computer Vision and Pattern Recognition (CVPR)*, 2021. **3, 8, 14**
- [9] Inseop Chung, Daesik Kim, and Nojun Kwak. Maximizing cosine similarity between spatial features for unsupervised domain adaptation in semantic segmentation. In *Proceedings of the IEEE/CVF Winter Conference on Applications of Computer Vision (WACV)*, 2022. **12, 13**
- [10] MMSegmentation Contributors. MMSegmentation: Openmmlab semantic segmentation toolbox and benchmark. <https://github.com/open-mmlab/mms Segmentation>, 2020. **5**
- [11] Marius Cordts, Mohamed Omran, Sebastian Ramos, Timo Rehfeld, Markus Enzweiler, Rodrigo Benenson, Uwe Franke, Stefan Roth, and Bernt Schiele. The cityscapes dataset for semantic urban scene understanding. In *Proceedings of the IEEE/CVF Conference on Computer Vision and Pattern Recognition (CVPR)*, 2016. **1, 2, 5, 8**
- [12] Alexey Dosovitskiy, Lucas Beyer, Alexander Kolesnikov, Dirk Weissenborn, Xiaohua Zhai, Thomas Unterthiner, Mostafa Dehghani, Matthias Minderer, Georg Heigold, Sylvain Gelly, et al. An image is worth 16x16 words: Transformers for image recognition at scale. In *International Conference on Learning Representations (ICLR)*, 2020. **6**
- [13] Qi Dou, Daniel Coelho de Castro, Konstantinos Kamnitsas, and Ben Glocker. Domain generalization via model-agnostic learning of semantic features. *Advances in Neural Information Processing Systems (NeurIPS)*, 2019. **3**
- [14] Ye Du, Yujun Shen, Haochen Wang, Jingjing Fei, Wei Li, Liwei Wu, Rui Zhao, Zehua Fu, and Qingjie Liu. Learning from future: A novel self-training framework for semantic segmentation. *Advances in Neural Information Processing Systems (NeurIPS)*, 2022. **2, 3, 6**
- [15] Mark Everingham, Luc Van Gool, Christopher KI Williams, John Winn, and Andrew Zisserman. The pascal visual object classes (voc) challenge. *International Journal of Computer Vision (IJCV)*, 2010. **2**
- [16] Yaroslav Ganin, Evgeniya Ustinova, Hana Ajakan, Pascal Germain, Hugo Larochelle, Fran ois Laviolette, Mario Marchand, and Victor Lempitsky. Domain-adversarial training of neural networks. *Journal of Machine Learning Research (JMLR)*, 2016. **2**
- [17] Ian Goodfellow, Jean Pouget-Abadie, Mehdi Mirza, Bing Xu, David Warde-Farley, Sherjil Ozair, Aaron Courville, and Yoshua Bengio. Generative adversarial nets. *Advances in Neural Information Processing Systems (NeurIPS)*, 2014. **2**
- [18] Kaiming He, Haoqi Fan, Yuxin Wu, Saining Xie, and Ross Girshick. Momentum contrast for unsupervised visual representation learning. In *Proceedings of the IEEE/CVF Conference on Computer Vision and Pattern Recognition (CVPR)*, 2020. **4, 14**
- [19] Kaiming He, Xiangyu Zhang, Shaoqing Ren, and Jian Sun. Deep residual learning for image recognition. In *Proceedings of the IEEE/CVF Conference on Computer Vision and Pattern Recognition (CVPR)*, 2016. **5, 6, 7, 12, 13, 15**
- [20] Judy Hoffman, Eric Tzeng, Taesung Park, Jun-Yan Zhu, Phillip Isola, Kate Saenko, Alexei Efros, and Trevor Darrell. Cycada: Cycle-consistent adversarial domain adaptation. In *International Conference on Machine Learning (ICML)*, 2018. **2, 8, 12, 13**
- [21] Judy Hoffman, Dequan Wang, Fisher Yu, and Trevor Darrell. Fcns in the wild: Pixel-level adversarial and constraint-based adaptation. *arXiv preprint arXiv:1612.02649*, 2016. **2**
- [22] Weixiang Hong, Zhenzhen Wang, Ming Yang, and Junsong Yuan. Conditional generative adversarial network for structured domain adaptation. In *Proceedings of the IEEE/CVF Conference on Computer Vision and Pattern Recognition (CVPR)*, 2018. **2**
- [23] Lukas Hoyer, Dengxin Dai, and Luc Van Gool. Daformer: Improving network architectures and training strategies for domain-adaptive semantic segmentation. In *Proceedings of the IEEE/CVF Conference on Computer Vision and Pattern Recognition (CVPR)*, 2022. **1, 3, 5, 6, 7, 8, 12, 14, 15, 16, 17**
- [24] Lukas Hoyer, Dengxin Dai, and Luc Van Gool. Hrda: Context-aware high-resolution domain-adaptive semantic segmentation. In *European Conference on Computer Vision (ECCV)*, 2022. **2, 6**
- [25] Lei Huang, Yi Zhou, Fan Zhu, Li Liu, and Ling Shao. Iterative normalization: Beyond standardization towards efficient whitening. In *Proceedings of the IEEE/CVF Conference on Computer Vision and Pattern Recognition (CVPR)*, 2019. **3**

[26] Guoliang Kang, Yunchao Wei, Yi Yang, Yuetong Zhuang, and Alexander Hauptmann. Pixel-level cycle association: A new perspective for domain adaptive semantic segmentation. *Advances in Neural Information Processing Systems (NeurIPS)*, 2020. 1, 12, 13

[27] Jogendra Nath Kundu, Akshay Kulkarni, Amit Singh, Varun Jampani, and R Venkatesh Babu. Generalize then adapt: Source-free domain adaptive semantic segmentation. In *Proceedings of the IEEE/CVF International Conference on Computer Vision (ICCV)*, 2021. 8

[28] Geoffrey Hinton Laurens Van der Maaten. Visualizing data using t-sne. *Journal of Machine Learning Research (JMLR)*, 2008. 17

[29] Yann LeCun, Bernhard Boser, John S Denker, Donnie Henderson, Richard E Howard, Wayne Hubbard, and Lawrence D Jackel. Backpropagation applied to handwritten zip code recognition. *Neural Computation*, 1989. 6

[30] Chen-Yu Lee, Tanmay Batra, Mohammad Haris Baig, and Daniel Ulbricht. Sliced wasserstein discrepancy for unsupervised domain adaptation. In *Proceedings of the IEEE/CVF Conference on Computer Vision and Pattern Recognition (CVPR)*, 2019. 2

[31] Da Li, Yongxin Yang, Yi-Zhe Song, and Timothy M Hospedales. Learning to generalize: Meta-learning for domain generalization. In *Proceedings of the AAAI Conference on Artificial Intelligence (AAAI)*, 2018. 3

[32] Da Li, Jianshu Zhang, Yongxin Yang, Cong Liu, Yi-Zhe Song, and Timothy M Hospedales. Episodic training for domain generalization. In *Proceedings of the IEEE/CVF International Conference on Computer Vision (ICCV)*, 2019. 3

[33] Haoliang Li, Sinno Jialin Pan, Shiqi Wang, and Alex C Kot. Domain generalization with adversarial feature learning. In *Proceedings of the IEEE/CVF Conference on Computer Vision and Pattern Recognition (CVPR)*, 2018. 3

[34] Ruihuang Li, Shuai Li, Chenhang He, Yabin Zhang, Xu Jia, and Lei Zhang. Class-balanced pixel-level self-labeling for domain adaptive semantic segmentation. In *Proceedings of the IEEE/CVF Conference on Computer Vision and Pattern Recognition (CVPR)*, 2022. 2, 3, 12, 13

[35] Ya Li, Xinmei Tian, Mingming Gong, Yajing Liu, Tongliang Liu, Kun Zhang, and Dacheng Tao. Deep domain generalization via conditional invariant adversarial networks. In *European Conference on Computer Vision (ECCV)*, 2018. 3

[36] Yiyi Li, Yongxin Yang, Wei Zhou, and Timothy Hospedales. Feature-critic networks for heterogeneous domain generalization. In *International Conference on Machine Learning (ICML)*, 2019. 3

[37] Yunsheng Li, Lu Yuan, and Nuno Vasconcelos. Bidirectional learning for domain adaptation of semantic segmentation. In *Proceedings of the IEEE/CVF Conference on Computer Vision and Pattern Recognition (CVPR)*, 2019. 2

[38] Qing Lian, Fengmao Lv, Lixin Duan, and Boqing Gong. Constructing self-motivated pyramid curriculums for cross-domain semantic segmentation: A non-adversarial approach. In *Proceedings of the IEEE/CVF International Conference on Computer Vision (ICCV)*, 2019. 1, 13

[39] Jonathan Long, Evan Shelhamer, and Trevor Darrell. Fully convolutional networks for semantic segmentation. In *Proceedings of the IEEE/CVF Conference on Computer Vision and Pattern Recognition (CVPR)*, 2015. 1

[40] Mingsheng Long, Yue Cao, Jianmin Wang, and Michael Jordan. Learning transferable features with deep adaptation networks. In *International Conference on Machine Learning (ICML)*, 2015. 2

[41] Mingsheng Long, Zhangjie Cao, Jianmin Wang, and Michael I Jordan. Conditional adversarial domain adaptation. *Advances in Neural Information Processing Systems (NeurIPS)*, 2018. 2

[42] Ilya Loshchilov and Frank Hutter. Decoupled weight decay regularization. In *International Conference on Learning Representations (ICLR)*, 2019. 5

[43] Yawei Luo, Ping Liu, Liang Zheng, Tao Guan, Junqing Yu, and Yi Yang. Category-level adversarial adaptation for semantic segmentation using purified features. *IEEE Transactions on Pattern Analysis and Machine Intelligence (TPAMI)*, 2021. 2

[44] Yawei Luo, Liang Zheng, Tao Guan, Junqing Yu, and Yi Yang. Taking a closer look at domain shift: Category-level adversaries for semantics consistent domain adaptation. In *Proceedings of the IEEE/CVF Conference on Computer Vision and Pattern Recognition (CVPR)*, 2019. 2

[45] Fengmao Lv, Tao Liang, Xiang Chen, and Guosheng Lin. Cross-domain semantic segmentation via domain-invariant interactive relation transfer. In *Proceedings of the IEEE/CVF Conference on Computer Vision and Pattern Recognition (CVPR)*, 2020. 13

[46] Ke Mei, Chuang Zhu, Jiaqi Zou, and Shanghang Zhang. Instance adaptive self-training for unsupervised domain adaptation. In *European Conference on Computer Vision (ECCV)*, 2020. 12, 13

[47] Saeid Motian, Marco Piccirilli, Donald A Adjeroh, and Gianfranco Doretto. Unified deep supervised domain adaptation and generalization. In *Proceedings of the IEEE/CVF International Conference on Computer Vision (ICCV)*, 2017. 3

[48] Zak Murez, Soheil Kolouri, David Kriegman, Ravi Ramamoorthi, and Kyungnam Kim. Image to image translation for domain adaptation. In *Proceedings of the IEEE/CVF Conference on Computer Vision and Pattern Recognition (CVPR)*, 2018. 2

[49] Sebastian Nowozin, Botond Cseke, and Ryota Tomioka. f-gan: Training generative neural samplers using variational divergence minimization. *Advances in Neural Information Processing Systems (NeurIPS)*, 2016. 2

[50] Viktor Olsson, Wilhelm Tranheden, Juliano Pinto, and Lennart Svensson. Classmix: Segmentation-based data augmentation for semi-supervised learning. In *Proceedings of the IEEE/CVF Conference on Computer Vision and Pattern Recognition (CVPR)*, 2021. 12

[51] Aaron van den Oord, Yazhe Li, and Oriol Vinyals. Representation learning with contrastive predictive coding. *arXiv preprint arXiv:1807.03748*, 2018. 3, 4

[52] Fei Pan, Inkyu Shin, Francois Fleuret, Seokju Lee, and In So Kweon. Unsupervised intra-domain adaptation for semantic segmentation through self-supervision. In *Proceedings of the IEEE/CVF Conference on Computer Vision and Pattern Recognition (CVPR)*, 2020. 2

[53] Xingang Pan, Ping Luo, Jianping Shi, and Xiaou Tang. Two at once: Enhancing learning and generalization capacities via ibn-net. In *European Conference on Computer Vision (ECCV)*, 2018. 3

[54] Adam Paszke, Sam Gross, Francisco Massa, Adam Lerer, James Bradbury, Gregory Chanan, Trevor Killeen, Zeming Lin, Natalia Gimelshein, Luca Antiga, et al. PyTorch: An imperative style, high-performance deep learning library. *Advances in Neural Information Processing Systems (NeurIPS)*, 2019. 5

[55] Mohammad Mahfujur Rahman, Clinton Fookes, Mahsa Baktashmotlagh, and Sridha Sridharan. Correlation-aware adversarial domain adaptation and generalization. *Pattern Recognition*, 2020. 3

[56] Stephan R Richter, Vibhav Vineet, Stefan Roth, and Vladlen Koltun. Playing for data: Ground truth from computer games. In *European Conference on Computer Vision (ECCV)*, 2016. 1, 2, 5

[57] Olaf Ronneberger, Philipp Fischer, and Thomas Brox. U-net: Convolutional networks for biomedical image segmentation. In *International Conference on Medical image computing and computer-assisted intervention*, 2015. 1

[58] German Ros, Laura Sellart, Joanna Materzynska, David Vazquez, and Antonio M Lopez. The synthia dataset: A large collection of synthetic images for semantic segmentation of urban scenes. In *Proceedings of the IEEE/CVF Conference on Computer Vision and Pattern Recognition (CVPR)*, 2016. 1, 2, 5

[59] Kuniaki Saito, Kohei Watanabe, Yoshitaka Ushiku, and Tatsuya Harada. Maximum classifier discrepancy for unsupervised domain adaptation. In *Proceedings of the IEEE/CVF Conference on Computer Vision and Pattern Recognition (CVPR)*, 2018. 2

[60] Swami Sankaranarayanan, Yogesh Balaji, Arpit Jain, Ser Nam Lim, and Rama Chellappa. Learning from synthetic data: Addressing domain shift for semantic segmentation. In *Proceedings of the IEEE/CVF Conference on Computer Vision and Pattern Recognition (CVPR)*, 2018. 2

[61] Inkyu Shin, Sanghyun Woo, Fei Pan, and In So Kweon. Two-phase pseudo label densification for self-training based domain adaptation. In *European Conference on Computer Vision (ECCV)*, 2020. 2

[62] Jong-Chyi Su, Subhransu Maji, and Bharath Hariharan. When does self-supervision improve few-shot learning? In *European Conference on Computer Vision (ECCV)*, 2020. 14

[63] Antti Tarvainen and Harri Valpola. Mean teachers are better role models: Weight-averaged consistency targets improve semi-supervised deep learning results. *Advances in Neural Information Processing Systems (NeurIPS)*, 2017. 3

[64] Wilhelm Tranheden, Viktor Olsson, Juliano Pinto, and Lennart Svensson. Dacs: Domain adaptation via cross-domain mixed sampling. In *Proceedings of the IEEE/CVF Winter Conference on Applications of Computer Vision (WACV)*, 2021. 2, 5, 12, 13

[65] Yi-Hsuan Tsai, Wei-Chih Hung, Samuel Schulter, Kihyuk Sohn, Ming-Hsuan Yang, and Manmohan Chandraker. Learning to adapt structured output space for semantic segmentation. In *Proceedings of the IEEE/CVF Conference on Computer Vision and Pattern Recognition (CVPR)*, 2018. 2, 12, 13

[66] Yi-Hsuan Tsai, Kihyuk Sohn, Samuel Schulter, and Manmohan Chandraker. Domain adaptation for structured output via discriminative patch representations. In *Proceedings of the IEEE/CVF International Conference on Computer Vision (ICCV)*, 2019. 2

[67] Tuan-Hung Vu, Himalaya Jain, Maxime Bucher, Matthieu Cord, and Patrick Pérez. Advent: Adversarial entropy minimization for domain adaptation in semantic segmentation. In *Proceedings of the IEEE/CVF Conference on Computer Vision and Pattern Recognition (CVPR)*, 2019. 1, 12, 13

[68] Haoran Wang, Tong Shen, Wei Zhang, Ling-Yu Duan, and Tao Mei. Classes matter: A fine-grained adversarial approach to cross-domain semantic segmentation. In *European Conference on Computer Vision (ECCV)*, 2020. 7, 8, 12, 13

[69] Haochen Wang, Kaiyou Song, Junsong Fan, Yuxi Wang, Jin Xie, and Zhaoxiang Zhang. Hard patches mining for masked image modeling. In *Proceedings of the IEEE/CVF Conference on Computer Vision and Pattern Recognition (CVPR)*, 2023. 3, 14

[70] Yuchao Wang, Jingjing Fei, Haochen Wang, Wei Li, Liwei Wu, Rui Zhao, and Yujun Shen. Balancing logit variation for long-tail semantic segmentation. In *Proceedings of the IEEE/CVF Conference on Computer Vision and Pattern Recognition (CVPR)*, 2023. 2

[71] Yuxi Wang, Junran Peng, and ZhaoXiang Zhang. Uncertainty-aware pseudo label refinery for domain adaptive semantic segmentation. In *Proceedings of the IEEE/CVF International Conference on Computer Vision (ICCV)*, 2021. 8

[72] Yuchao Wang, Haochen Wang, Yujun Shen, Jingjing Fei, Wei Li, Guoqiang Jin, Liwei Wu, Rui Zhao, and Xinyi Le. Semi-supervised semantic segmentation using unreliable pseudo labels. In *Proceedings of the IEEE/CVF Conference on Computer Vision and Pattern Recognition (CVPR)*, 2022. 4, 13

[73] Zhonghao Wang, Mo Yu, Yunchao Wei, Rogerio Feris, Jinjun Xiong, Wen-mei Hwu, Thomas S Huang, and Honghui Shi. Differential treatment for stuff and things: A simple unsupervised domain adaptation method for semantic segmentation. In *Proceedings of the IEEE/CVF Conference on Computer Vision and Pattern Recognition (CVPR)*, 2020. 2

[74] Binhui Xie, Shuang Li, Mingjia Li, Chi Harold Liu, Gao Huang, and Guoren Wang. Sepico: Semantic-guided pixel contrast for domain adaptive semantic segmentation. *IEEE Transactions on Pattern Analysis and Machine Intelligence (TPAMI)*, 2023. 2, 7, 8

[75] Enze Xie, Wenhui Wang, Zhiding Yu, Anima Anandkumar, Jose M Alvarez, and Ping Luo. Segformer: Simple and efficient design for semantic segmentation with transformers. *Advances in Neural Information Processing Systems (NeurIPS)*, 2021. 5, 6, 7, 15

[76] Jinyu Yang, Weizhi An, Sheng Wang, Xinliang Zhu, Chaochao Yan, and Junzhou Huang. Label-driven reconstruction for domain adaptation in semantic segmentation. In *European Conference on Computer Vision (ECCV)*, 2020. 2

[77] Yanchao Yang and Stefano Soatto. Fda: Fourier domain adaptation for semantic segmentation. In *Proceedings of the IEEE/CVF Conference on Computer Vision and Pattern Recognition (CVPR)*, 2020. 2, 3, 5, 6, 7, 8, 9, 13

[78] Pan Zhang, Bo Zhang, Ting Zhang, Dong Chen, Yong Wang, and Fang Wen. Prototypical pseudo label denoising and target structure learning for domain adaptive semantic segmentation. In *Proceedings of the IEEE/CVF Conference on Computer Vision and Pattern Recognition (CVPR)*, 2021. 2, 3, 6, 12, 13

[79] Qiming Zhang, Jing Zhang, Wei Liu, and Dacheng Tao. Category anchor-guided unsupervised domain adaptation for semantic segmentation. *Advances in Neural Information Processing Systems (NeurIPS)*, 2019. 1, 2, 12, 13

[80] Hengshuang Zhao, Jianping Shi, Xiaojuan Qi, Xiaogang Wang, and Jiaya Jia. Pyramid scene parsing network. In *Proceedings of the IEEE/CVF Conference on Computer Vision and Pattern Recognition (CVPR)*, 2017. 1

[81] Zhedong Zheng and Yi Yang. Rectifying pseudo label learning via uncertainty estimation for domain adaptive semantic segmentation. *International Journal of Computer Vision (IJCV)*, 2021. 2

[82] Bolei Zhou, Hang Zhao, Xavier Puig, Sanja Fidler, Adela Barriuso, and Antonio Torralba. Scene parsing through ade20k dataset. In *Proceedings of the IEEE/CVF Conference on Computer Vision and Pattern Recognition (CVPR)*, 2017. 1

[83] Qianyu Zhou, Chuyun Zhuang, Xuequan Lu, and Lizhuang Ma. Domain adaptive semantic segmentation with regional contrastive consistency regularization. In *Proceedings of the IEEE International Conference on Multimedia and Expo (ICME)*, 2022. 12, 13

[84] Yang Zou, Zhiding Yu, BVK Kumar, and Jinsong Wang. Unsupervised domain adaptation for semantic segmentation via class-balanced self-training. In *European Conference on Computer Vision (ECCV)*, 2018. 1, 2, 5, 12, 13

[85] Yang Zou, Zhiding Yu, Xiaofeng Liu, BVK Kumar, and Jinsong Wang. Confidence regularized self-training. In *Proceedings of the IEEE/CVF Conference on Computer Vision and Pattern Recognition (CVPR)*, 2019. 2, 5

Supplementary Material

In this supplementary material, we first provide more details in Sec. A. Later, we give an extended comparison with more UDA methods with ResNet-101 [19] and DeepLab-V2 [5] on both GTA5 → Cityscapes and SYNTHIA → Cityscapes benchmarks in Sec. B. Moreover, in Sec. C, we conduct extra ablation studies. We further evaluate the performance on source domain in Sec. D to find out whether T2S-DA is able to maintain a capable source feature space during training. In Sec. E, we visualize the feature space of 1) the source only baseline, 2) DAFormer, and 3) our T2S-DA to verify pulling target to source indeed urges the model to learn similar cross-domain features, rather than self-training. Sec. F gives a visualization of segmentation maps provided by the source only baseline, DAFormer [23], and our T2S-DA evaluated on GTA5 → Cityscapes. Finally, we discuss the broader impact and potential negative impact and provide the pseudo-code for computing contrastive loss in Sec. G.

A. More Details

Details for Target Loss. For unlabeled target data, we adopt self-training, which minimizes the weighted cross-entropy loss between predictions and pseudo-labels \hat{y}^t generated by the teacher.

$$\mathcal{L}_{\text{target}} = \sum_{i=1}^{n_t} \sum_{j=1}^{H \times W} q_i^t \cdot \ell_{ce} [f_s \circ h_s(\mathbf{x}_i^t)(j), \hat{y}_i^t(j)], \quad (\text{S1})$$

where $\hat{y}_i^t(j)$ is the one-hot pseudo-label generated by the teacher for i -th target image at position j . Moreover, following [23] and [64], we use q_i^t the ratio of pixels whose softmax probability exceeds a threshold δ_p to be the metric to measure the quality of pseudo-labels of the i -th target image:

$$q_i^t = \frac{1}{H \times W} \sum_{j=1}^{H \times W} \mathbb{1}[\max_c f_t \circ h_t(\mathbf{x}_i^t) > \delta_p], \quad (\text{S2})$$

where $\mathbb{1}[\cdot]$ is the indicator function and δ_p is set to 0.968 following [64].

Details for data augmentation. We follow DACS [64], using color jitter, Gaussian blur, and ClassMix [50] to be a strong augmentation to make self-training more efficient.

Details in Fig. 1. Category-wise similarities for cross-domain *centroids* are provided in Fig. 1. To be specific, we first compute the centroid (prototype) for each category on both source and target domains. Next, cosine similarity is computed across domains.

B. Extended Comparison

We extend the comparison of T2S-DA with previous UDA methods from the main paper by a large selection of further methods for GTA5 → Cityscapes in Tab. S1 and for SYNTHIA → Cityscapes in Tab. S2. Selected methods can be summarized to three mainstreams: 1) adversarial training based methods for domain alignment, including AdaptSeg [65], CyCADA [20], ADVENT [67], FADA [68], 2) self-training based approaches, including CBST [84], IAST [46], CAG [79], ProDA [78], SAC [1], CPSL [34], and 3) contrastive learning based alternatives, including PLCA [26], RCCR [83], and MCS [9]. All methods in Tab. S1 and Tab. S2 are based on DeepLab-V2 [5] with ResNet-101 [19] as backbone. Note that, we report the performances of ProDA [78] and CPSL [34] in Tab. S1 and Tab. S2 without knowledge distillation using self-supervised trained models for a fair comparison. Our proposed method outperforms other competitors by a large margin, achieving mIoU of 60.4% on GTA5 → Cityscapes, and 57.6% over 16 classes and 65.4% over 13 classes on SYNTHIA → Cityscapes, respectively. Especially for class “sidewalk” on GTA5 → Cityscapes and class “bike” on SYNTHIA → Cityscapes, T2S-DA achieves IoU scores of 73.4% and 62.6%, outperforming the second place by +13.0% and +8.5% respectively.

Compared with other contrastive learning based methods PLCA [26], MCS [9], and RCCR [83], our T2S-DA outperforms them by a large margin on both GTA5 → Cityscapes and SYNTHIA → Cityscapes. This indicates the efficiency of urging the model to make target features as similar to source features as possible, leading to a more cross-domain category-discriminative feature space of our T2S-DA.

C. Ablation Studies

C.1. Ablation Studies with CNN-based Models

We conduct experiments in Tab. S3 and Tab. S4 with CNN-based models. We take DACS [64] with two extra training strategies proposed by DAFormer [23] as the baseline. From Tab. S3 and Tab. S4, we can get similar conclusions to Transformer-based models. First, both vanilla contrast on source domain and pulling source to target, *i.e.*, “source → target”, bring limited improvements. Additionally, introducing an image translation engine does alleviate the false positive issue in conducting positive pairs, but the improvements are still limited when pulling source to target. *Only when pulling target to source*, it outperforms the baseline significantly. Dynamic re-weighting cannot be applied to cross-entropy loss directly owing to the greater domain shift and noisier pseudo-labels that underperforming classes are suffered from.

Table S1. Comparison with state-of-the-art alternatives on **GTA5** → **Cityscapes** benchmark with ResNet-101 [19] and DeepLab-V2 [5]. The results are averaged over 3 random seeds. The top performance is highlighted in **bold** font and the second score is *underlined*.

Method	Road	S.walk	Build.	Wall	Fence	Pole	T.light	Sign	Veget.	Terrain	Sky	Person	Rider	Car	Truck	Bus	Train	M.bike	Bike	mIoU
source only	70.2	14.6	71.3	24.1	15.3	25.5	32.1	13.5	82.9	25.1	78.0	56.2	33.3	76.3	26.6	29.8	12.3	28.5	18.0	38.6
AdaptSeg [65]	86.5	36.0	79.9	23.4	23.3	23.9	35.2	14.8	83.4	33.3	75.6	58.5	27.6	73.7	32.5	35.4	3.9	30.1	28.1	41.4
CyCADA [20]	86.7	35.6	80.1	19.8	17.5	38.0	39.9	41.5	82.7	27.9	73.6	64.9	19.0	65.0	12.0	28.6	4.5	31.1	42.0	42.7
ADVENT [67]	89.4	33.1	81.0	26.6	26.8	27.2	33.5	24.7	83.9	36.7	78.8	58.7	30.5	84.8	38.5	44.5	1.7	31.6	32.4	45.5
CBST [84]	91.8	53.5	80.5	32.7	21.0	34.0	28.9	20.4	83.9	34.2	80.9	53.1	24.0	82.7	30.3	35.9	16.0	25.9	42.8	45.9
PCLA [26]	84.0	30.4	82.4	35.3	24.8	32.2	36.8	24.5	85.5	37.2	78.6	66.9	32.8	85.5	40.4	48.0	8.8	29.8	41.8	47.7
FADA [68]	92.5	47.5	85.1	37.6	32.8	33.4	33.8	18.4	85.3	37.7	83.5	63.2	39.7	87.5	32.9	47.8	1.6	34.9	39.5	49.2
MCS [9]	92.6	54.0	85.4	35.0	26.0	32.4	41.2	29.7	85.1	40.9	85.4	62.6	34.7	85.7	35.6	50.8	2.4	31.0	34.0	49.7
CAG [79]	90.4	51.6	83.8	34.2	27.8	38.4	25.3	48.4	85.4	38.2	78.1	58.6	34.6	84.7	21.9	42.7	41.1	29.3	37.2	50.2
FDA [77]	92.5	53.3	82.4	26.5	27.6	36.4	40.6	38.9	82.3	39.8	78.0	62.6	34.4	84.9	34.1	53.1	16.9	27.7	46.4	50.5
PIT [45]	87.5	43.4	78.8	31.2	30.2	36.3	39.3	42.0	79.2	37.1	79.3	65.4	37.5	83.2	<u>46.0</u>	45.6	<u>25.7</u>	23.5	49.9	50.6
IAST [46]	93.8	57.8	85.1	39.5	26.7	26.2	43.1	34.7	84.9	32.9	88.0	62.6	29.0	87.3	39.2	49.6	23.2	34.7	39.6	51.5
DACS [64]	89.9	39.7	87.9	30.7	39.5	38.5	46.4	<u>52.8</u>	<u>88.0</u>	<u>44.0</u>	88.8	67.2	35.8	84.5	45.7	50.2	0.0	27.3	34.0	52.1
RCCR [83]	93.7	<u>60.4</u>	86.5	41.1	32.0	37.3	38.7	38.6	87.2	43.0	85.5	65.4	35.1	<u>88.3</u>	41.8	51.6	0.0	38.0	52.1	53.5
ProDA [78]	91.5	52.4	82.9	42.0	<u>35.7</u>	40.0	44.4	43.3	87.0	43.8	79.5	66.5	31.4	86.7	41.1	52.5	0.0	45.4	<u>53.8</u>	53.7
CPSL [34]	91.7	52.9	83.6	<u>43.0</u>	32.3	43.7	<u>51.3</u>	42.8	85.4	37.6	81.1	<u>69.5</u>	30.0	88.1	44.1	59.9	24.9	<u>47.2</u>	48.4	<u>55.7</u>
T2S-DA (ours)	96.2	73.4	88.6	45.1	37.4	<u>40.7</u>	54.0	55.5	88.9	48.6	<u>88.2</u>	72.2	45.0	89.6	53.8	<u>56.2</u>	1.3	53.0	59.6	60.4

Table S2. Comparison with state-of-the-art alternatives on **SYNTHIA** → **Cityscapes** benchmark with ResNet-101 [19] and DeepLab-V2 [5]. The results are averaged over 3 random seeds. The mIoU and the mIoU* indicate we compute mean IoU over 16 and 13 categories, respectively. The top performance is highlighted in **bold** font and the second score is *underlined*.

Method	Road	S.walk	Build.	Wall*	Fence*	Pole*	T.light	Sign	Veget.	Sky	Person	Rider	Car	Bus	M.bike	Bike	mIoU	mIoU*
source only [†]	55.6	23.8	74.6	9.2	0.2	24.4	6.1	12.1	74.8	79.0	55.3	19.1	39.6	23.3	13.7	25.0	33.5	38.6
AdaptSeg [65]	79.2	37.2	78.8	-	-	-	9.9	10.5	78.2	80.5	53.5	19.6	67.0	29.5	21.6	31.3	-	45.9
ADVENT [67]	85.6	42.2	79.7	8.7	0.4	25.9	5.4	8.1	80.4	84.1	57.9	23.8	73.3	36.4	14.2	33.0	41.2	48.0
CBST [84]	68.0	29.9	76.3	10.8	1.4	33.9	22.8	29.5	77.6	78.3	60.6	28.3	81.6	23.5	18.8	39.8	42.6	48.9
CAG [79]	84.7	40.8	81.7	7.8	0.0	35.1	13.3	22.7	84.5	77.6	64.2	27.8	80.9	19.7	22.7	48.3	44.5	51.5
PIT [45]	83.1	27.6	81.5	8.9	0.3	21.8	26.4	33.8	76.4	78.8	64.2	27.6	79.6	31.2	31.0	31.3	44.0	51.8
FDA [77]	79.3	35.0	73.2	-	-	-	19.9	24.0	61.7	82.6	61.4	31.1	83.9	40.8	38.4	51.1	-	52.5
FADA [68]	84.5	40.1	83.1	4.8	0.0	34.3	20.1	27.2	84.8	84.0	53.5	22.6	85.4	43.7	26.8	27.8	45.2	52.5
MCS [9]	<u>88.3</u>	47.3	80.1	-	-	-	21.6	20.2	79.6	82.1	59.0	28.2	82.0	39.2	17.3	46.7	-	53.2
PyCDA [38]	75.5	30.9	83.3	20.8	0.7	32.7	27.3	33.5	84.7	85.0	64.1	25.4	85.0	45.2	21.2	32.0	46.7	53.3
PLCA [26]	82.6	29.0	81.0	11.2	0.2	33.6	24.9	18.3	82.8	82.3	62.1	26.5	85.6	48.9	26.8	52.2	46.8	54.0
DACS [64]	80.6	25.1	81.9	21.5	<u>2.9</u>	37.2	22.7	24.0	83.7	90.8	67.6	<u>38.3</u>	82.9	38.9	28.5	47.6	48.3	54.8
RCCR [83]	79.4	45.3	83.3	-	-	-	24.7	29.6	68.9	87.5	63.1	33.8	87.0	51.0	32.1	52.1	-	56.8
IAST [46]	81.9	41.5	83.3	17.7	4.6	32.3	30.9	28.8	83.4	85.0	65.5	30.8	86.5	38.2	33.1	52.7	49.8	57.0
ProDA [78]	87.1	44.0	83.2	26.9	0.7	42.0	45.8	<u>34.2</u>	<u>86.7</u>	81.3	68.4	22.1	<u>87.7</u>	50.0	31.4	38.6	51.9	58.5
SAC [1]	89.3	<u>47.2</u>	<u>85.5</u>	<u>26.5</u>	1.3	43.0	45.5	32.0	87.1	<u>89.3</u>	63.6	25.4	86.9	35.6	30.4	53.0	52.6	59.3
CPSL [34]	87.3	44.4	83.8	<u>25.0</u>	0.4	42.9	<u>47.5</u>	32.4	86.5	83.3	<u>69.6</u>	29.1	89.4	<u>52.1</u>	<u>42.6</u>	<u>54.1</u>	<u>54.4</u>	<u>61.7</u>
T2S-DA (ours)	81.2	38.3	86.0	<u>26.5</u>	1.8	43.8	48.0	54.6	85.2	86.6	73.0	40.8	87.5	52.8	52.2	62.6	57.6	65.4

C.2. Detailed Ablations of Dynamic Re-Weighting

To further verify the efficiency of dynamic re-weighting on long-tailed classes, we conduct experiments in Tab. S5. We provide per-class results on GTA5 to Cityscapes benchmark in the following Table. We choose 9 classes with the least training samples in the Cityscapes dataset as tail classes, *i.e.*, wall, traffic light, traffic sign, rider, truck, bus, train, motorcycle, and bicycle. As shown in Tab. S5, dynamic re-weighting obtains significant improvements on tail classes with both CNN-based models and Transformer-based models.

For simple re-weighting (SRW), following previous works [72] evaluated on Cityscapes, we use [0.8373, 0.918, 0.866, 1.0345, 1.0166, 0.9969, 0.9754, 1.0489, 0.8786, 1.0023, 0.9539, 0.9843, 1.1116, 0.9037, 1.0865, 1.0955, 1.0865, 1.1529, 1.0507] as the weight of each class, replacing w_c^* in Eq. (2). DRW outperforms SRW by +1.0% mIoU and +0.9% mIoU on tail classes with CNN-based models and Transformer-based models, respectively.

Table S3. **Ablation study** on the way of constructing contrastive pairs and computing loss with CNN-based models.

case	CE	Que.	Pos.	Neg.	mIoU
baseline	src.	-	-	-	56.3 \pm 0.4
vanilla contrast	src.	src.	src.	src.	57.5 \pm 1.2
source \rightarrow target	src.	src.	trg.	src. + trg.	57.3 \pm 0.9
source \rightarrow p. target	src.	src.	p. trg.	src. + trg.	58.4 \pm 1.4
p. target \rightarrow source	src.	p. trg.	src.	src.	60.1 \pm 0.4
T2S-DA	src.	p. trg.	src.	src. + trg.	60.4\pm0.6
p. target \rightarrow source	p. trg.	p. trg.	src.	src. + trg.	58.7 \pm 0.4

Table S4. **Ablation study** on each component adopted by our framework with CNN-based models.

$\mathcal{L}_{\text{pull}}$	PT	CBQS	DRW	DENPS	mIoU
			✓		56.3 \pm 0.4
✓		✓	✓	✓	56.9 \pm 0.6
✓	✓				57.3 \pm 0.9
✓	✓	✓			59.0 \pm 1.5
✓	✓	✓	✓		59.2 \pm 0.2
✓	✓	✓	✓	✓	59.8 \pm 0.6
✓	✓	✓	✓	✓	60.4\pm0.6

C.3. Ablations of Hyper-Parameters

Ablation of λ . Tab. S6 shows the performances of our T2S-DA with different weight of contrastive loss λ , among which $\lambda = 0.1$ performs the best. When λ is too small (*i.e.*, 0.01), the performance is close to the baseline, indicating that the target features are still undesirable, while when λ is too large (*i.e.*, 1), the model tends to pay too much attention on learning similar features across domains rather than focus on the particular downstream task: semantic segmentation.

Ablation of τ . Tab. S7 ablates the tunable temperature parameter τ introduced in Eq. (2). We find that $\tau = 0.2$ achieves the best performance. One potential reason is that a smaller τ provides less difficulty in matching the correct positive key, while a larger τ results in too strict criteria for this dictionary look-up pretext task, which is similar to having a large contrastive loss weight λ .

Ablation of β . Tab. S8 studies the scale parameter of dynamic re-weighting described in Eq. (9), where $\beta = 0.5$ yields slightly better performance, indicating that dynamic re-weighting is quite robust against β .

Ablation of α . Tab. S9 ablates the unreliable partition α introduced in Eq. (7), which is used to filter unreliable predictions on the target domain to be candidate negative pairs. As illustrated, $\alpha = 50\%$ achieves slightly better performance, and our T2S-DA is insensitive to α .

Ablation of n and m . Tab. S10 studies the base number of queries per class n and the total number negative pairs per query m introduced in Sec. 3.3. We find that $n = 128$ and $m = 1024$ yield slightly better performance. Therefore, our framework is found to be stable to different n and m .

D. Performance on Source Domain

As our proposed T2S-DA tries to make target features as similar to source features as possible, leading to a category-discriminative feature representation space on target domain, which implicitly assumes the model will *not* deteriorate and is able to maintain a capable feature space on the source domain during training. Therefore, we conduct experiments in Tab. S11 to verify this assumption. We do not find a significant gap between three methods (source only baseline, DAFormer [23], and our proposed T2S-DA).

E. Analysis on Feature Space

Fig. S1 gives a visualization of feature spaces of 1) the source only baseline, 2) DAFormer [23], and 3) our proposed T2S-DA, where their source features are discriminative enough but target features for source only baseline and DAFormer [23] run into chaos, while our proposed T2S-DA is able to build a category-discriminative feature space. This indicates that only by self-training as DAFormer [23] does, target features are not capable enough. By urging the model to learn similar cross-domain features, our proposed T2S-DA makes the decision boundary lies in low-density regions.

F. Qualitative Results

From Fig. S2, we can tell that T2S-DA is able to distinguish the conjunction of “rider” and “bike/motorbike”, benefiting from pushing features for different categories away. From Fig. S3, we can tell that T2S-DA can bootstrap the performance on categories with large cross-domain feature dissimilarities (*i.e.*, “bus” in Fig. 1), indicating that T2S-DA is able to extract domain-invariant feature representations which leads to better performance. From Fig. S4, we can tell that T2S-DA pays more attention to underperforming categories, *i.e.*, “pole” and “sign” where the IoU scores of source only baseline are 34.5% and 23.4% respectively (see Tab. 1), thanks to dynamic re-weighting.

G. Discussion and Pseudo-Code

Broader Impact. Our proposed T2S-DA framework has been proven to be efficient in building discriminative feature representation space on the unlabeled target domain by urging the model to extract similar cross-domain features for each category. Therefore, our work provides a new perspective for improving the robustness of neural networks, and is able to be applied in domain generalization [8], few-shot learning [62], and unsupervised representations learning [18, 69].

Potential negative impact. Our work is economically friendly and may have a positive impact on saving labor costs in annotating dense segmentation maps, which makes

Table S5. Validation of dynamic re-weighting against simple re-weighting on long-tailed classes.

Method	Head Classes												Tail Classes											
	mIoU	mIoU (Tail)	Road	S.walk	Build.	Fence	Pole	Veget.	Terrain	Sky	Person	Car	Wall	Tlight	Sign	Rider	Truck	Bus	Train	M.bike	Bike			
<i>CNN-based</i>												DeepLab-V2 [5] with ResNet-101 [19]												
source only	38.6	24.2	70.2	14.6	71.3	15.3	25.5	82.9	25.1	78.0	56.2	76.3	24.1	32.1	13.5	33.3	26.6	29.8	12.3	28.5	18.0			
T2S-DA (w/o DRW)	59.2	45.0	95.6	71.0	88.8	36.0	41.8	89.2	47.3	87.2	73.4	90.2	41.1	54.9	56.8	47.5	49.4	58.1	0.0	41.8	55.5			
T2S-DA (w/ SRW)	59.6	45.8	95.8	71.1	88.8	35.8	41.5	88.8	47.7	88.0	73.4	89.7	42.5	55.1	56.8	46.7	48.4	56.8	0.0	49.1	57.1			
T2S-DA (w/ DRW)	60.4	46.8	96.2	73.4	88.6	37.4	40.7	88.9	48.6	88.2	72.2	89.6	45.1	54.0	55.5	45.0	53.8	56.2	1.3	51.0	59.6			
<i>Transformer-based</i>												DAFormer [23] with MiT-B5 [75]												
source only	46.1	29.9	76.1	18.7	84.6	31.4	34.5	87.5	42.6	87.3	63.4	81.1	29.8	44.8	23.4	21.2	39.3	44.6	2.9	33.2	29.7			
T2S-DA (w/o DRW)	68.9	62.0	95.7	59.4	89.9	43.7	52.6	90.7	50.1	92.9	74.5	92.5	51.8	61.5	61.5	46.2	63.6	80.1	68.4	58.7	65.8			
T2S-DA (w/ SRW)	69.2	62.8	95.0	66.7	89.6	45.4	51.5	90.5	50.4	92.4	74.5	92.9	54.1	61.4	56.8	45.8	73.2	79.8	70.5	59.2	64.7			
T2S-DA (w/ DRW)	70.0	63.7	95.9	71.1	89.9	46.6	52.4	90.3	49.8	92.5	74.6	93.2	54.5	61.6	61.0	46.3	75.8	76.3	72.4	58.9	66.8			

Table S6. Study on contrastive loss weight λ .

λ	mIoU
0.01	68.3 \pm 0.9
0.1	70.0\pm0.6
0.5	68.2 \pm 0.6
1	67.3 \pm 0.4

Table S7. Study on temperature parameter τ .

τ	mIoU
0.02	69.3 \pm 0.4
0.2	70.0\pm0.6
0.5	68.8 \pm 0.7

Table S8. Study on re-weighting coefficient β .

β	mIoU
0.1	69.9 \pm 0.6
0.5	70.0\pm0.6
1	68.8 \pm 0.4

Table S9. Study on unreliable partition α .

α	mIoU
10%	69.5 \pm 0.1
50%	70.0\pm0.6
90%	69.4 \pm 0.5

Table S10. Study on the number of queries n and the number of negative pairs m .

n	m	mIoU
64	1024	68.7 \pm 0.3
128	1024	70.0\pm0.6
256	1024	69.3 \pm 0.5
128	512	69.5 \pm 0.5
128	2048	68.8 \pm 0.3

a segmentation model able to generalize from a synthetic labeled source domain to an unlabeled real-world target domain. All experiments are conducted on public datasets and are not involve sensitive attributes. However, as a general problem for semantic segmentation algorithms, our method might be used in undesired military applications such as unmanned aerial vehicles.

Pseudo-code of T2S-DA, *i.e.*, how to sample queries and keys, and then compute $\mathcal{L}_{\text{pull}}$, is provided in algorithm 1.

Table S11. Evaluation on **source domain** on GTA5 → Cityscapes benchmark.

Method	Road	S.walk	Build.	Wall	Fence	Pole	Tlight	Sign	Veget.	Terrain	Sky	Person	Rider	Car	Truck	Bus	Train	M.bike	Bike	mIoU
source only	97.6	89.7	91.8	72.4	58.9	66.2	66.6	68.1	86.1	76.1	96.6	79.8	70.0	92.7	90.8	94.4	87.5	73.7	53.9	79.6
DAFormer [23]	97.2	87.9	91.2	68.9	55.9	65.7	67.5	71.5	85.9	74.7	96.6	79.9	75.6	92.4	89.9	93.9	92.7	80.3	64.9	80.7
T2S-DA (ours)	97.2	88.1	91.3	69.2	57.0	66.6	68.2	71.4	86.0	74.8	96.6	79.7	76.0	92.4	90.2	94.7	91.2	80.4	64.7	80.9

Algorithm 1 Pseudo-code of T2S-DA in a PyTorch-like style.

```

1 # img_src, img_trg, img_ptrg: images of source, target, pseudo-target domain
2 # label_src: semantic label for img_src
3 # m_s, m_t: the student model and the teacher model
4
5 # num_cls, alpha: total number of classes, unreliable partition
6 # beta: scale factor for dynamic re-weighting
7 # n, m: base number of queries per class, number of negative keys per query
8
9 m_s.train()
10 m_t.eval()
11 pred_ptrg, feat_ptrg = m_s.forward(img_ptrg)
12 feat_ptrg = feat_ptrg / torch.norm(feat_ptrg, dim=1, keepdim=True) # 12-norm
13
14 with torch.no_grad():
15     pred_src, feat_src = m_t.forward(img_src)
16     pred_trg, feat_trg = m_t.forward(img_trg)
17     # 12-norm
18     feat_src = feat_src / torch.norm(feat_src, dim=1, keepdim=True)
19     feat_trg = feat_trg / torch.norm(feat_trg, dim=1, keepdim=True)
20     # get confidence and pseudo-label for target image
21     conf_trg, label_trg = torch.max(softmax(pred_trg, dim=1), dim=1)
22     # get confidence threshold
23     conf_thresh = np.percentile(conf_trg.numpy().flatten(), 100 * alpha)
24
25 # dynamic re-weighting
26 conf = [conf_trg[label_trg == cls].mean() for cls in range(num_cls)]
27 max_weight = torch.min(1 - conf)
28 weight = [(1 - conf[cls]) / max_weight) ** beta for cls in range(num_cls)]
29 weight /= weight.sum()
30
31 # compute source prototypes (positive keys)
32 prototype = [torch.mean(feat_src[label_src == cls], dim=0) for cls in range(num_cls)]
33
34 # estimate label distribution for sampling queries
35 distribution = [(label_src == cls).sum() for cls in range(num_cls)]
36 distribution /= distribution.sum()
37
38 # compute contrastive loss for each category
39 loss = 0
40 for cls in range(num_cls):
41     query_cls = feat_ptrg[label_src == cls]
42
43     # class-balanced query sampling
44     n_q = math.ceil(n * num_cls * distribution[cls])
45     index_q = np.random.choice(len(query_cls), n_q)
46     query_select = query_cls[index_q]
47
48     # domain-equalized negative pair sampling
49     neg_src = feat_src[(label_src != cls)]
50     neg_trg = feat_trg[(label_trg != cls) * (conf_trg < conf_thresh)]
51     src_idx = np.random.choice(len(neg_src), m // 2)
52     trg_idx = np.random.choice(len(neg_trg), m // 2)
53     neg_feat = torch.cat((neg_src[src_idx], neg_trg[trg_idx]), dim=0)
54
55     # compute logits
56     neg_logits = torch.matmul(query_select, neg_feat.T)
57     pos_logits = torch.matmul(query_select, prototype[cls].unsqueeze(1))
58     logits = torch.cat((pos_logits, neg_logits), dim=1)
59
60     # compute loss
61     labels = torch.zeros((len(logits),)).long()
62     loss += weight[cls] * (logits / tau, labels)

```

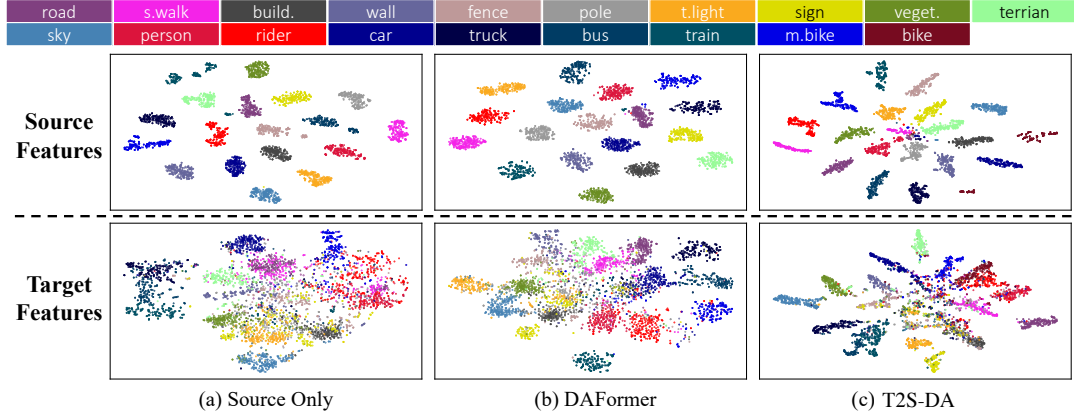


Figure S1. Comparison of the feature space using t-SNE [28] visualization between (a) the source only baseline, (b) DAFormer [23], and (c) our proposed T2S-DA. Note that we randomly sample 256 pixels for each category for better visualization.

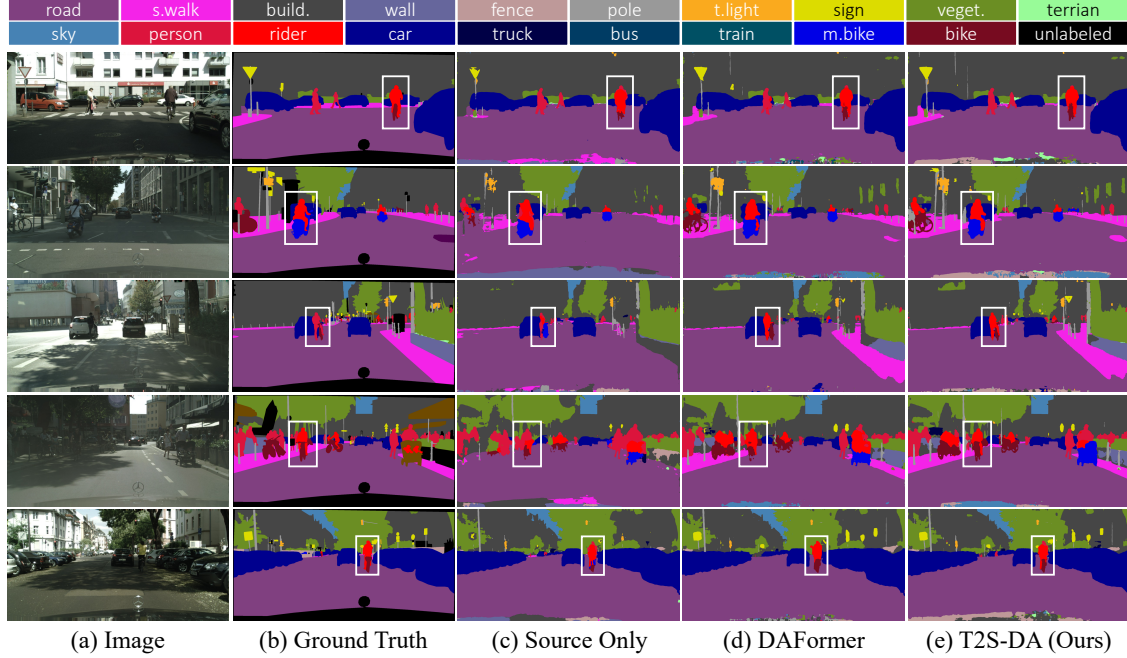


Figure S2. Example predictions showing better recognition and finer segmentation details of borders of “rider” and “bike/motorbike” on GTA5 → Cityscapes (best-viewed zoomed-in).

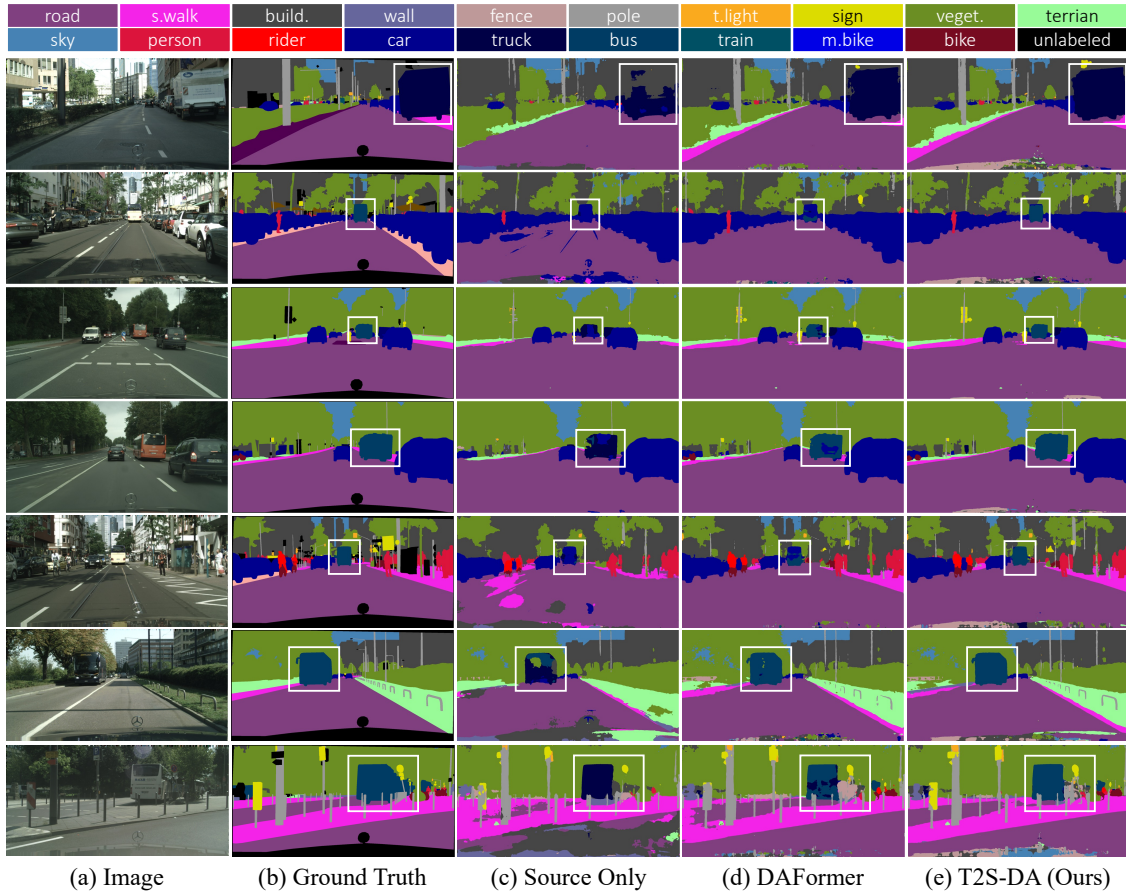


Figure S3. Example predictions showing a better recognition and finer segmentation details of “bus” and “truck” on GTA5 → Cityscapes, which are easily confused with a dominant category “car” (best-viewed zoomed-in).

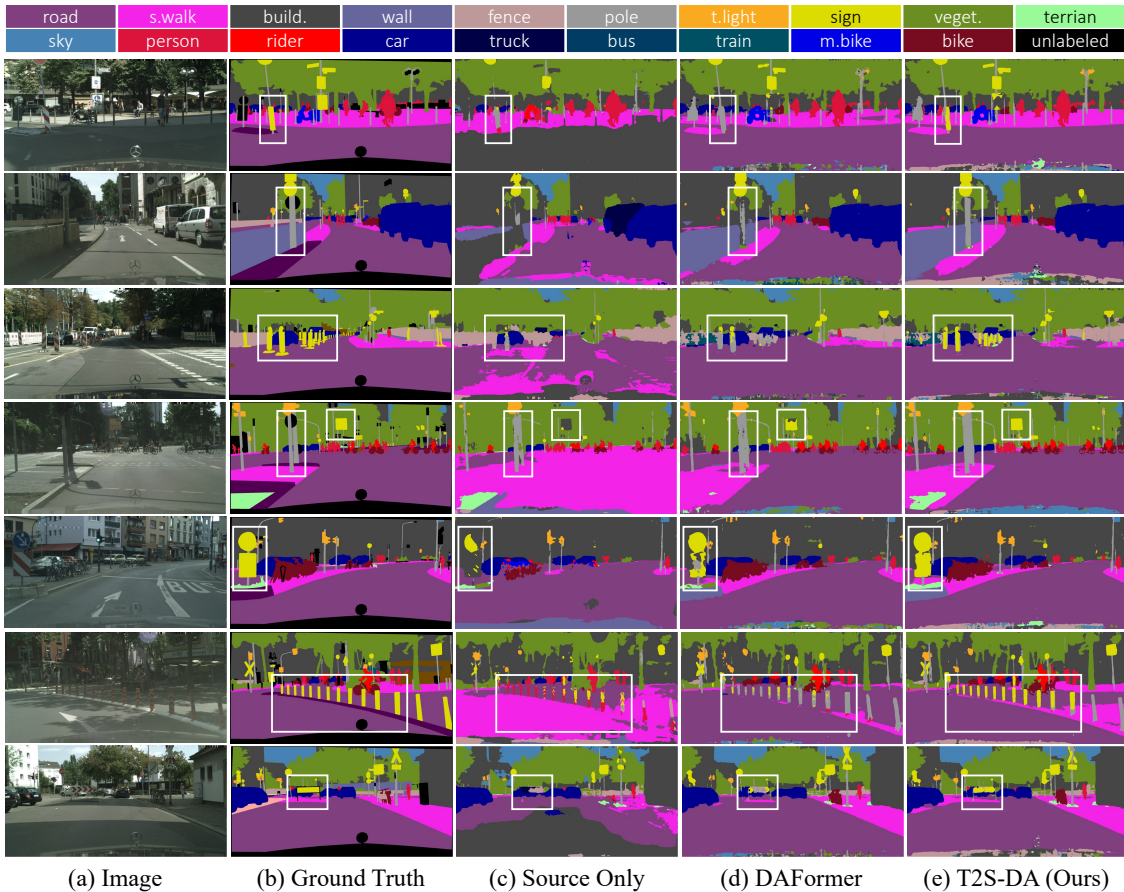


Figure S4. Example predictions showing better recognition and finer segmentation details of underperforming categories (“pole” and “sign”) on GTA5 → Cityscapes (best-viewed zoomed-in).